SPE SoAR

Sean Ford, Bill Walter, and Rob Mellors, LLNL

- Explosion Model Comparison
  - Canonical explosion models compared to SPE
- Moment Tensor Analysis
  - Inversion for SPE moment tensor solution
- Coda-wave Interferometry
  - Inferences on slowness perturbation due to SPE-2/-3
- Spall
  - Standard spall models compared to SPE

An Explosion Model Comparison with Insights from the Source Physics Experiment

Sean Ford and Bill Walter

SSA 2013

sean@llnl.gov

Lawrence Livermore National Laboratory is operated by Lawrence Livermore National Security, LLC, for the U.S. Department of Energy, National Nuclear Security Administration under Contract DE-AC52-07NA27344.

LLNL-PRES-635238

Motivation & Introduction

- Predict absolute ground motion for explosions using non-standard testing practice (i.e., not NTS or STS media at ~100 m/kT$^{1/3}$)

- Mueller & Murphy (1971) MM71
  - Scaling laws for seismic observables

- Denny & Johnson (1991) DJ91
  - Regression analysis for seismic observables

Previous work

- Denny (1998)
  - DOB
  - DJ91 f_c < observed

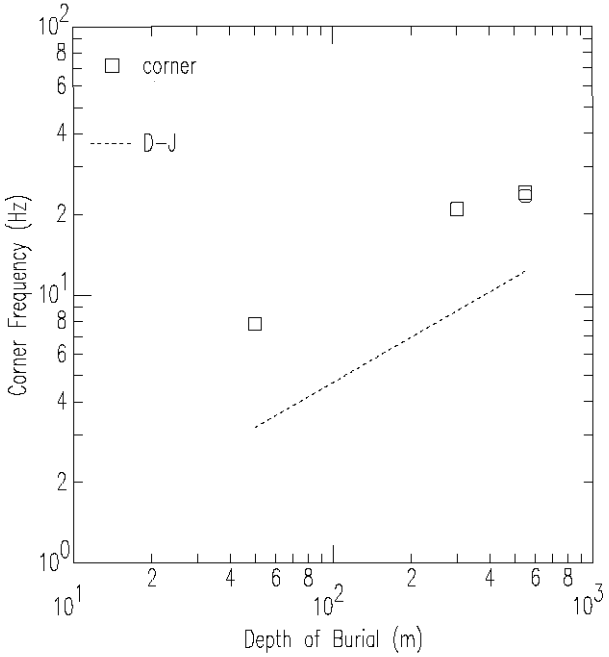

Previous work

- Denny (1998)
  - DOB
  - DJ91 f_c < observed
- Stump et al. (1999)
  - NPE
  - MM71 with $r_c \sim W^{1/3}$

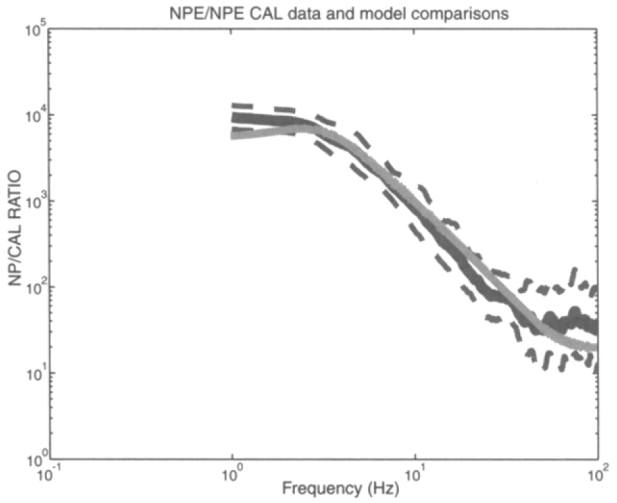

Previous work

- Denny (1998)
  - DOB
  - DJ91 f_c < observed
- Stump et al. (1999)
  - NPE
  - MM71 with $r_c \sim W^{1/3}$
- Rougier et al. (2011)
  - Simulation
  - DJ91 $r_c \cong$ predicted

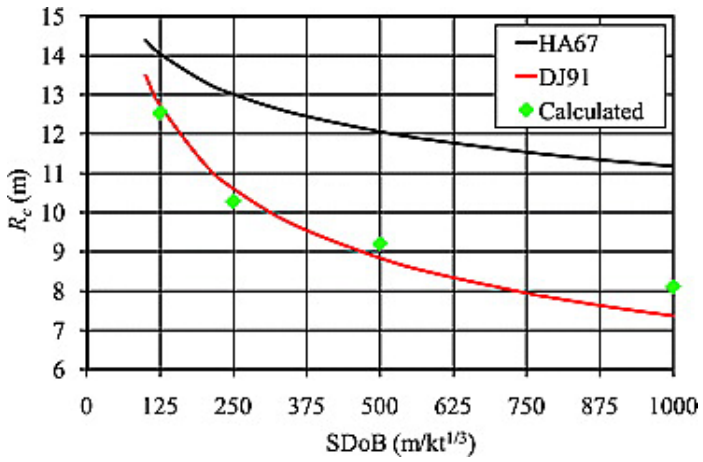

Model comparison (M_0)

- Denny & Johnson (1991) DJ91
  - Combine chem and nuke data in cavity regression where $r_c \sim W^{1/3}$ so $M_0 \sim W$
  - Relate cavity to "measured moment"

$$M_0^{DJ} = 4.2743 \times 10^{10} W \alpha^2 \beta^{-1.1544} P^{-0.4385} 10^{-0.0344 GP} \rho$$

Model comparison (M_0)

- Denny & Johnson (1991) DJ91
  - Combine chem and nuke data in cavity regression where $r_c \sim W^{1/3}$ so $M_0 \sim W$
  - Relate cavity to "measured moment"

$$M_0^{DJ} = 4.2743 \times 10^{10} W \alpha^2 \beta^{-1.1544} P^{-0.4385} 10^{-0.0344 GP} \rho$$

- Mueller & Murphy (1971) MM71
  - Assume scaling in amplitude and yield for nuke data
  - Employ a cavity regression where $r_c \sim W^{0.29}$ so $M_0 \sim W^{0.87}$

$$M_0^{MM} = 3.1416 W^{0.87} \alpha^2 \beta^{-2} R_0^3 P_0 h_0^{1/3} h^{-1/3}$$

Model comparison (f_c)

- DJ91 relate cavity to source radius with $\beta / \pi f_c$

$$f_c^{DJ} = 0.2045 W^{-1/3} \beta^{-0.0642} P^{0.5522} 10^{0.0025 GP} \rho^{-0.7245}$$

Model comparison (f_c)

- DJ91 relate cavity to source radius with $\beta / \pi f_c$

$$f_c^{DJ} = 0.2045 W^{-1/3} \beta^{-0.0642} P^{0.5522} 10^{0.0025 GP} \rho^{-0.7245}$$

- MM71 relate elastic radius to ω_0 with α / f_c

$$f_c^{MM} = 0.1592 W^{-1/3} \alpha R_0^{-1} h_0^{-1/n} h^{1/n}$$

Model comparison (f_c)

- DJ91 relate cavity to source radius with $\beta / \pi f_c$

$$f_c^{DJ} = 0.2045 W^{-1/3} \beta^{-0.0642} P^{0.5522} 10^{0.0025 GP} \rho^{-0.7245}$$

- MM71 relate elastic radius to ω_0 with α / f_c

$$f_c^{MM} = 0.1592 W^{-1/3} \alpha R_0^{-1} h_0^{-1/n} h^{1/n}$$

- DJ91/MM71 ~ f(DOB)
  - Allow for chem/nuke factor

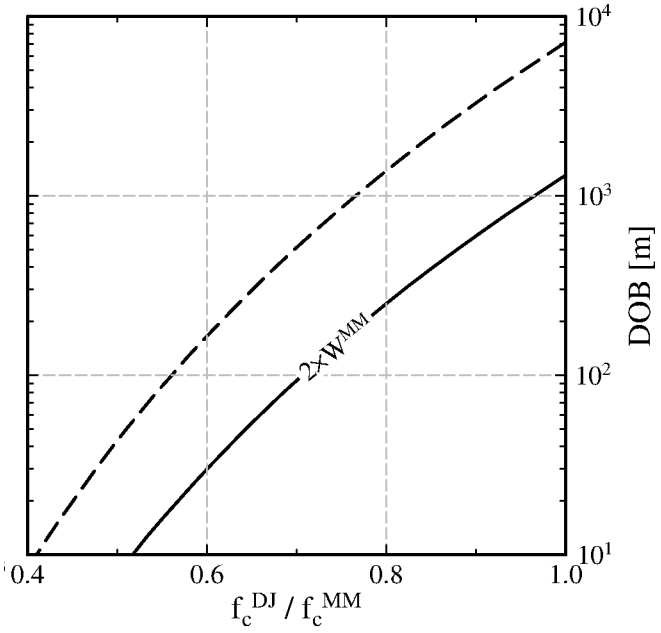

Model comparison (*W*)

- Invert DJ91 and MM71 M_0 relationship for yield

$$W^{DJ} = 2.940 \times 10^{-10} \beta^{1.1544} P^{0.4385} 10^{0.0344 GP} \Psi_{\infty}$$

$$W^{MM} = 4.9207 \rho^{1.1494} \beta^{2.2989} R_0^{-3.4483} P_0^{-1.1494} h_0^{-0.3831} h^{0.3831} \Psi_{\infty}^{1.1494}$$

Model comparison (*W*)

- Invert DJ91 and MM71 M_0 relationship for yield

$$W^{DJ} = 2.940 \times 10^{-10} \beta^{1.1544} P^{0.4385} 10^{0.0344GP} \Psi_\infty$$

$$W^{MM} = 4.9207 \rho^{1.1494} \beta^{2.2989} R_0^{-3.4483} P_0^{-1.1494} h_0^{-0.3831} h^{0.3831} \Psi_\infty^{1.1494}$$

  - Assume shot point ρ ~ overburden ρ $\quad \dfrac{W^{DJ}}{W^{MM}} = F \dfrac{h^{0.0554}}{M_0^{0.1494}}$

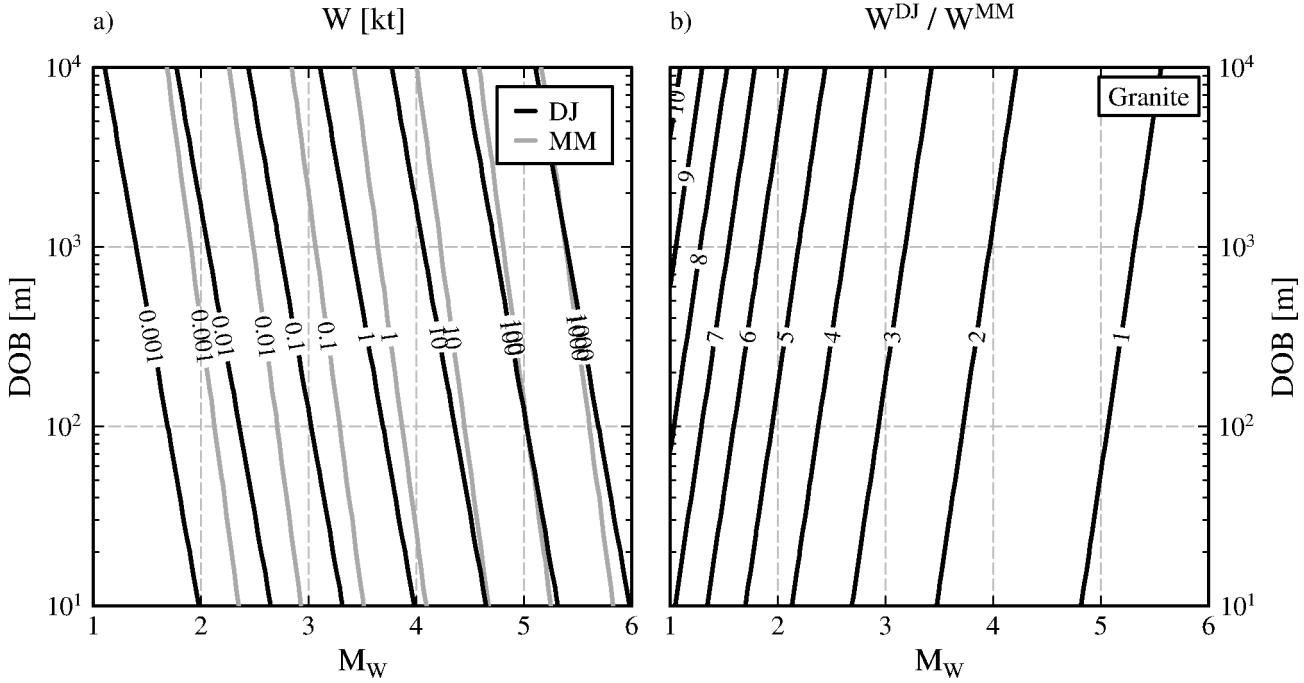

Model comparison (*W*)

- Invert DJ91 and MM71 M_0 relationship for yield

$$W^{DJ} = 2.940 \times 10^{-10} \beta^{1.1544} P^{0.4385} 10^{0.0344GP} \Psi_\infty$$

$$W^{MM} = 4.9207 \rho^{1.1494} \beta^{2.2989} R_0^{-3.4483} P_0^{-1.1494} h_0^{-0.3831} h^{0.3831} \Psi_\infty^{1.1494}$$

  - Assume shot point ρ ~ overburden ρ $\quad \dfrac{W^{DJ}}{W^{MM}} = F \dfrac{h^{0.0554}}{M_0^{0.1494}}$

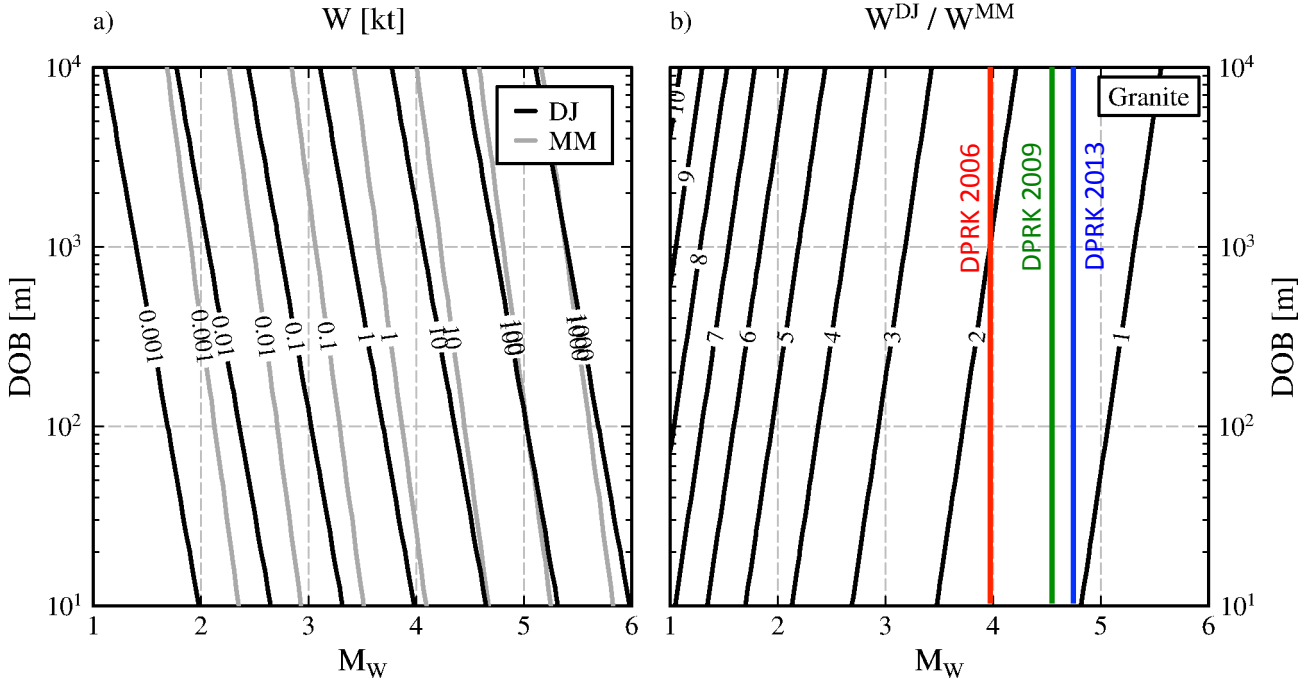

Model comparison (*W*)

- Invert DJ91 and MM71 M_0 relationship for yield

$$W^{DJ} = 2.940 \times 10^{-10} \beta^{1.1544} P^{0.4385} 10^{0.0344GP} \Psi_\infty$$

$$W^{MM} = 4.9207 \rho^{1.1494} \beta^{2.2989} R_0^{-3.4483} P_0^{-1.1494} h_0^{-0.3831} h^{0.3831} \Psi_\infty^{1.1494}$$

  - Assume shot point ρ ~ overburden ρ $\quad \dfrac{W^{DJ}}{W^{MM}} = F \dfrac{h^{0.0554}}{M_0^{0.1494}}$

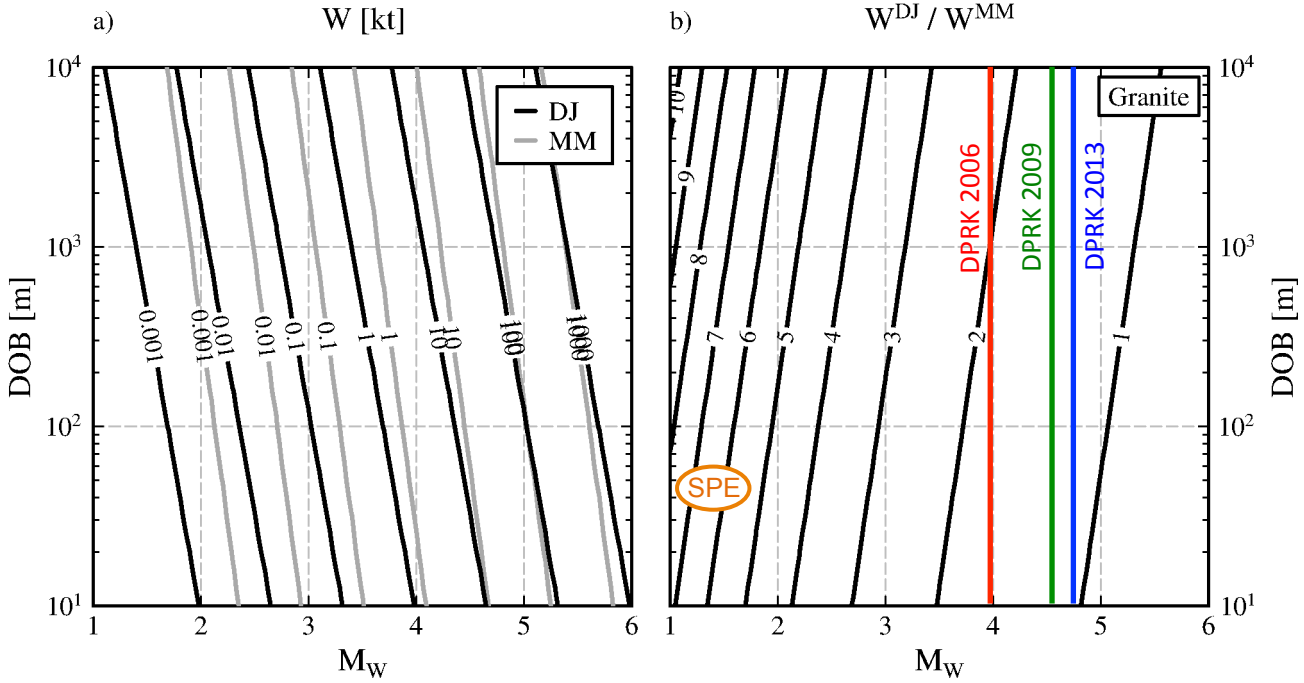

Data: SPE

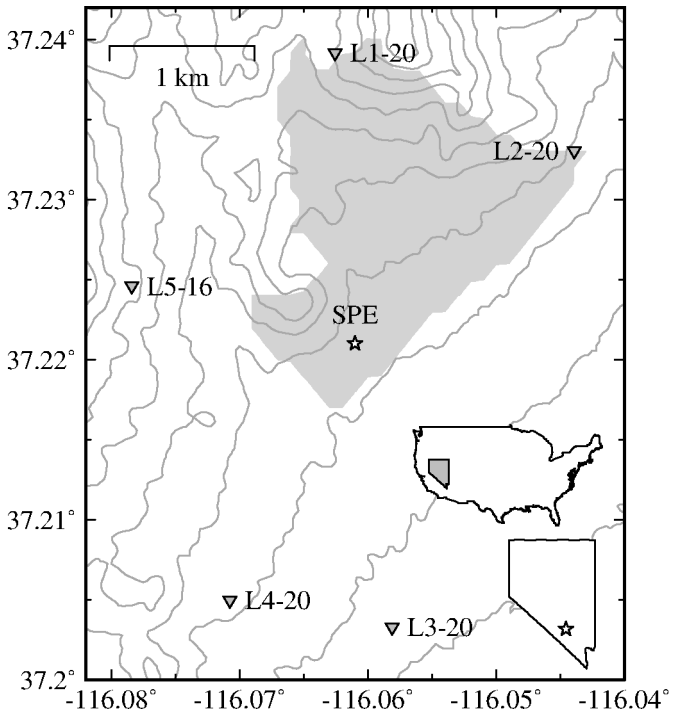

Shot	Yield [kg] (=TNT)	Depth [m]	sDOB [m/kT$^{1/3}$]
SPE-1	85.2	54.9	990
SPE-2	991.6	45.7	364

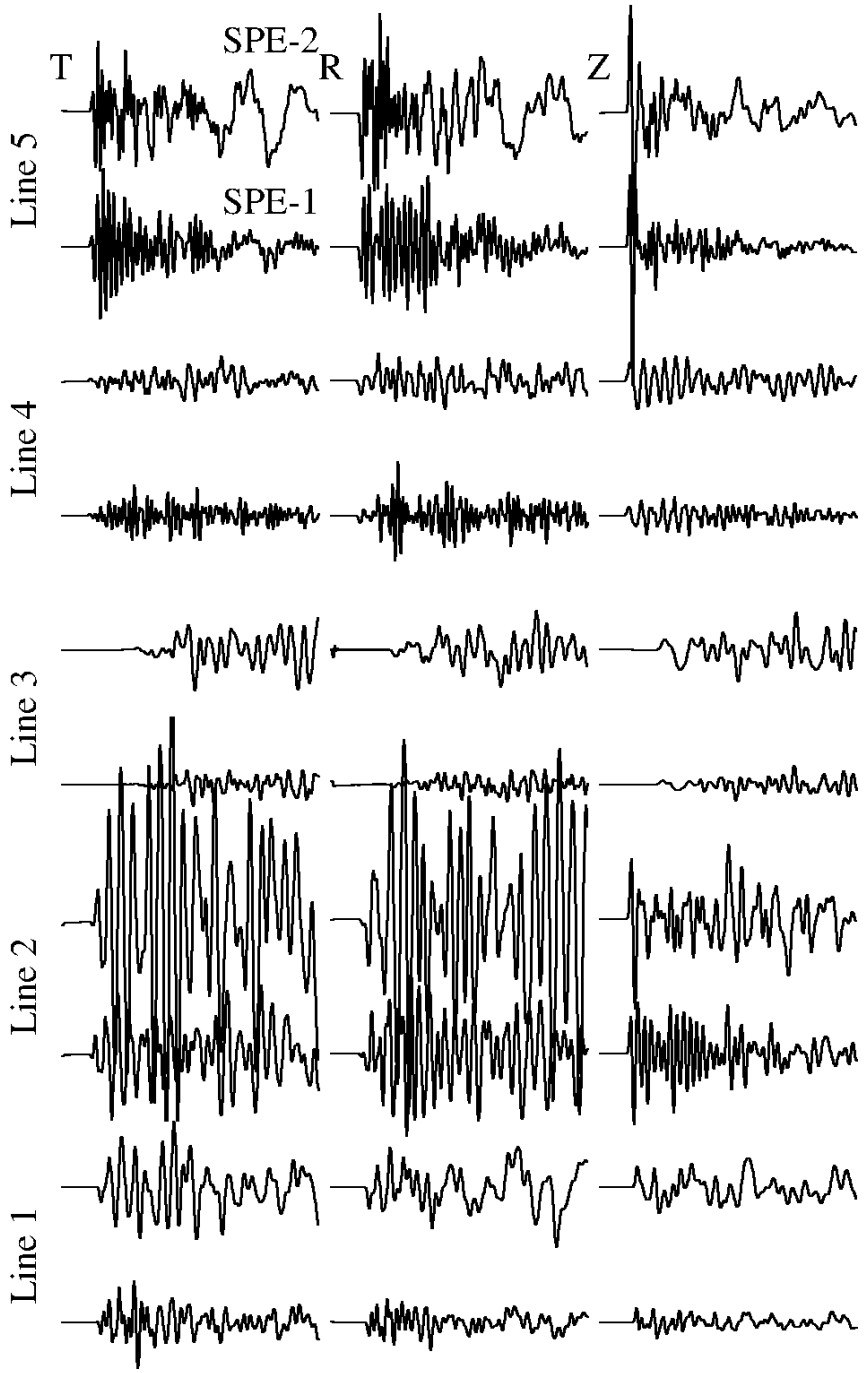

Relative comparison: Spectral ratio

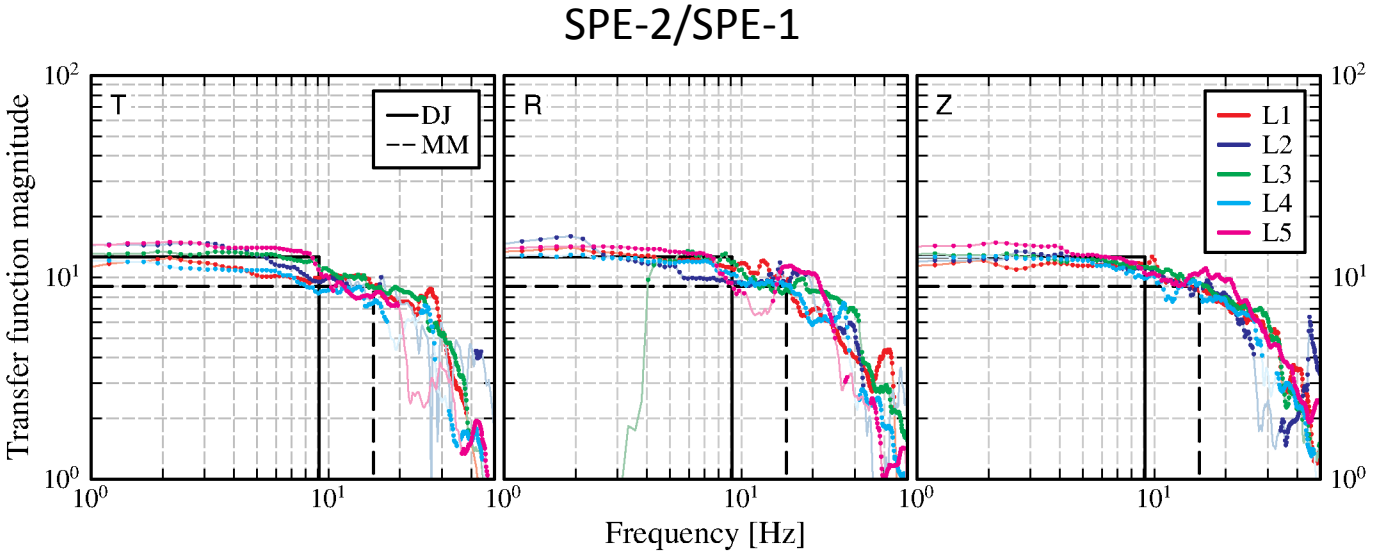

- MM under-predicts long period ratio
- DJ under-predicts corner-frequency

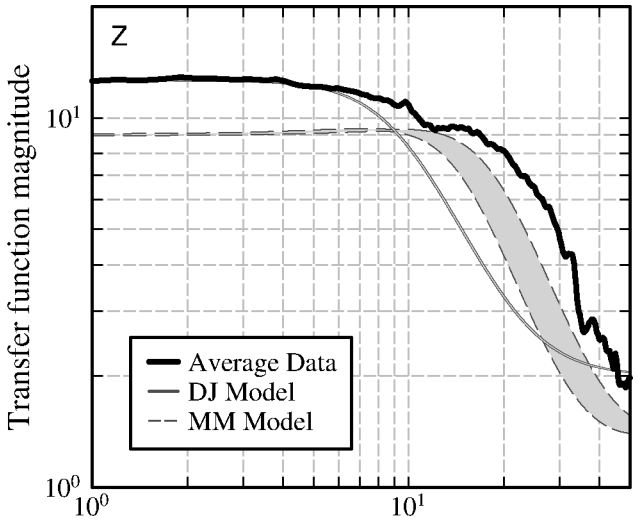

Relative comparison: Spectral ratio

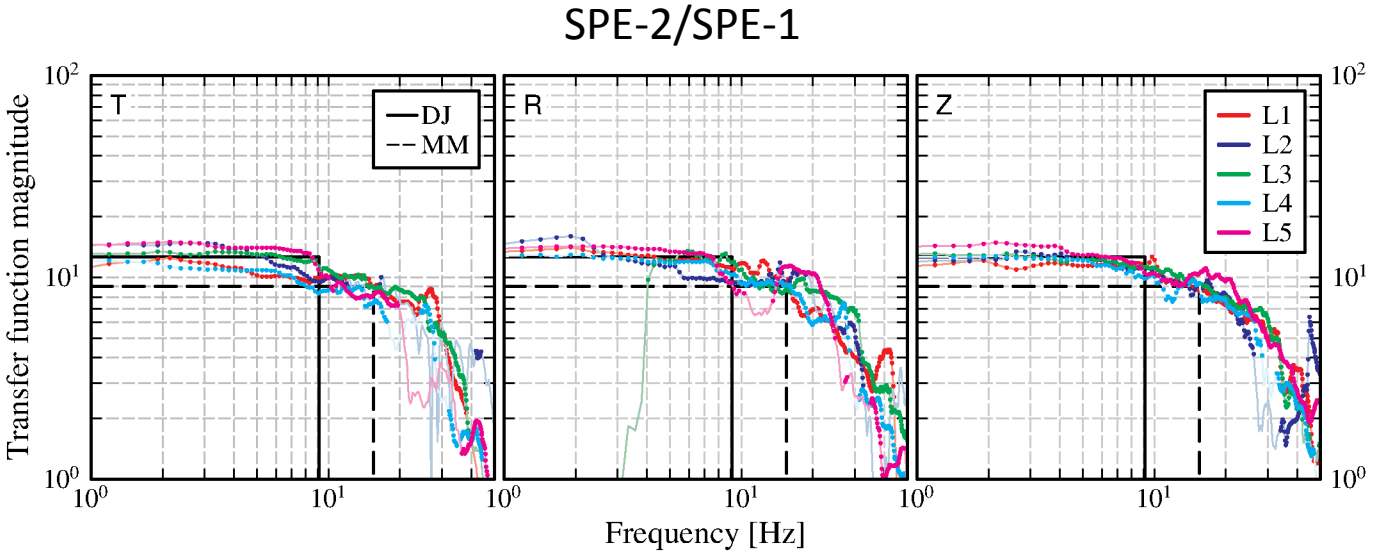

- Altering MM71 so that $r_c \sim W^{1/3}$ (Murphy & Barker, 1994) gives a better fit to the long-period ratio

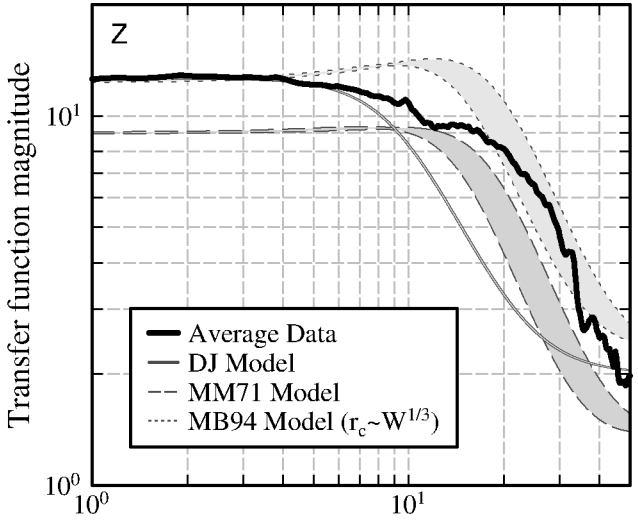

Absolute comparison: MT synthetic

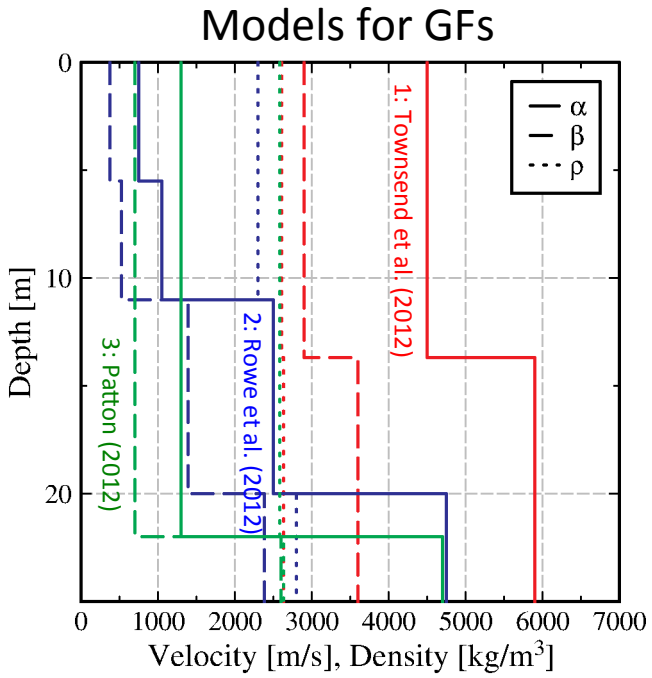

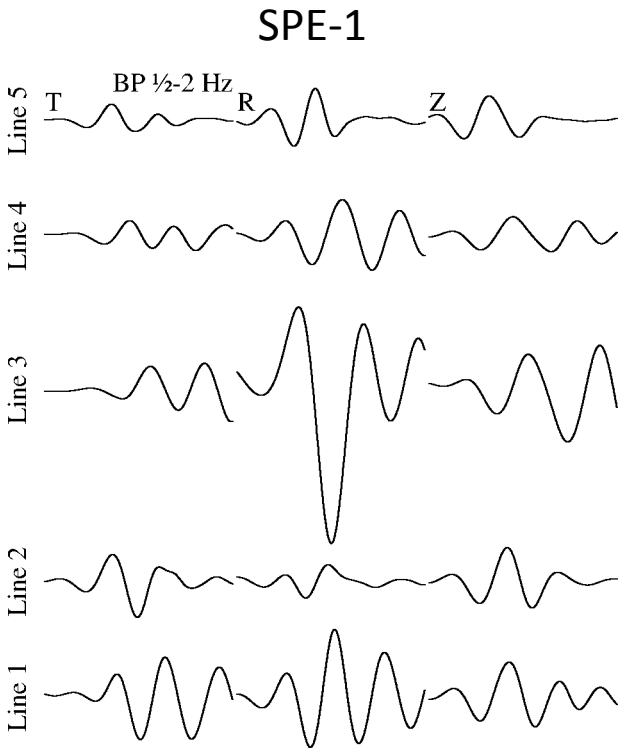

- Energy on tangential component
- Site effects along some lines

Absolute comparison: MT synthetic

Model	M_0^{DJ} [nAk]
1	48.5
2	52.5
3	44.8

Note: 1 Ak = 10^{18} N-m

SPE-1

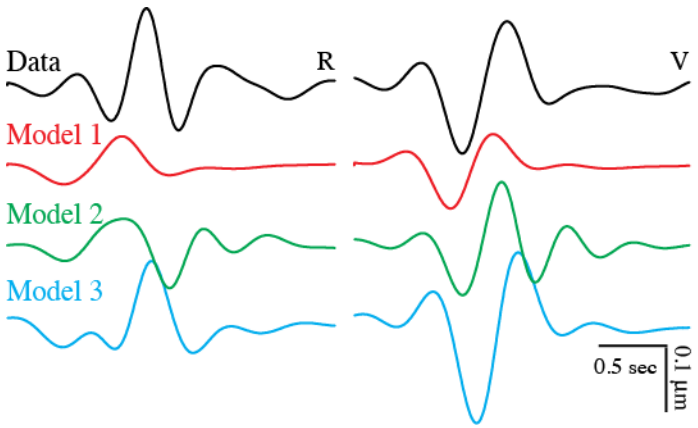

- DJ91 prediction near the observed displacement
- Best phase and amplitude fit by Model 3 (Patton, 2012)

Absolute comparison: MT synthetic

Model	M_0^{DJ} [nAk]	M_0^{MM} [nAk] 1×W	2×W
1	48.5	251.7	460.1
2	52.5	373.3	682.3
3	44.8	306.3	559.7

Note: 1 Ak = 10^{18} N-m

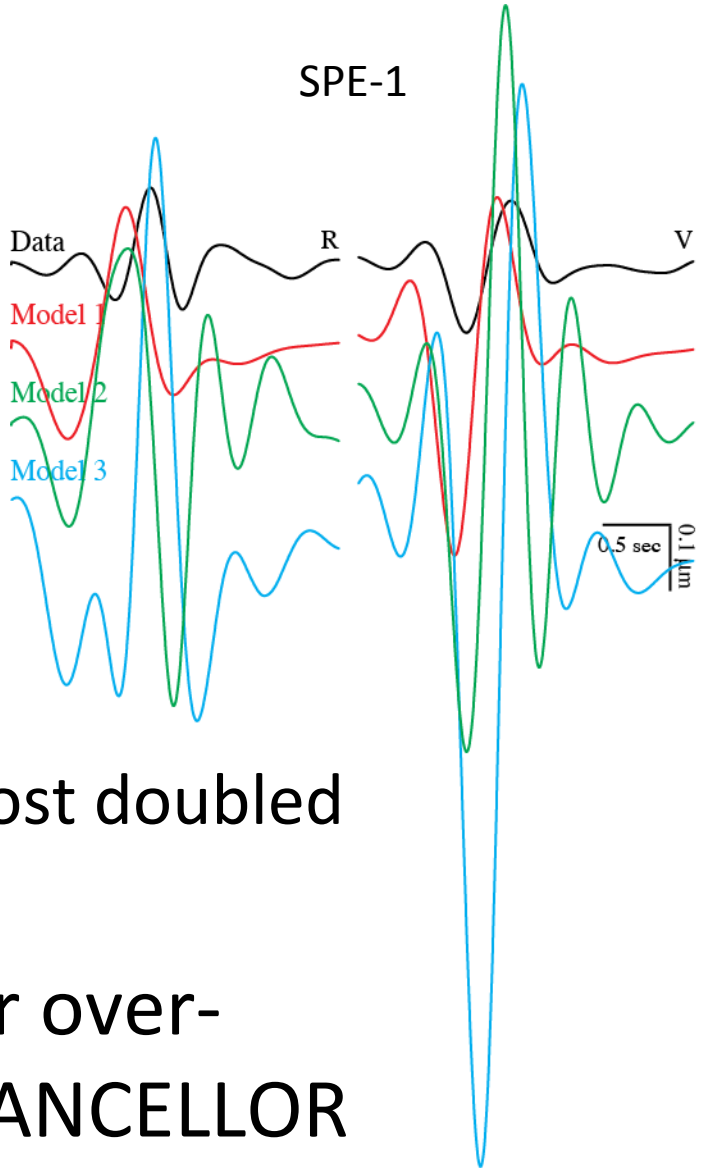

- MM71 over-predicts M_0
  - Synthetic amplitudes are almost doubled for chem/nuke factor = 2
- Johnson (1988) found similar over-prediction for HARZER & CHANCELLOR

Conclusions & Future work

- Differences in yield predictions are greatest for small and/or deeply buried explosions
- SPE is most consistent with D&J-predicted M_0 and M&M-predicted f_c

Conclusions & Future work

- Differences in yield predictions are greatest for small and/or deeply buried explosions
- SPE is most consistent with D&J-predicted M_0 and M&M-predicted f_c

- Future work: Chem/Nuke at depth (Xu et al., '12)

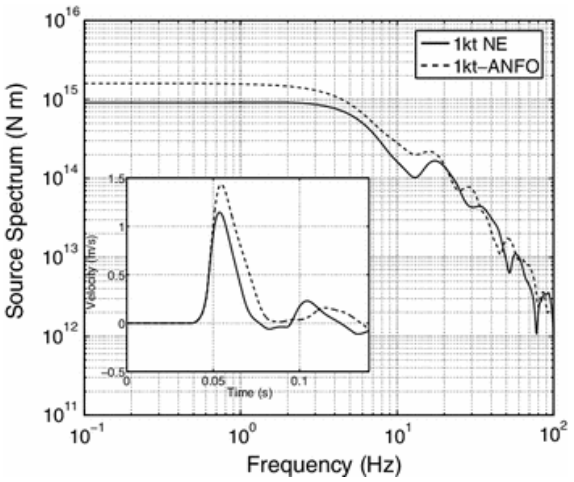

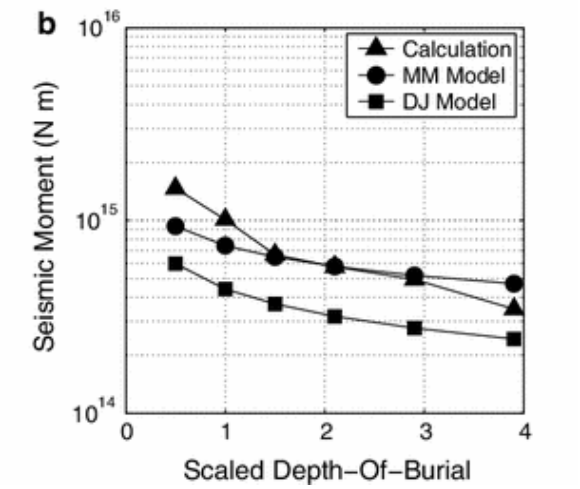

Conclusions & Future work

- Differences in yield predictions are greatest for small and/or deeply buried explosions
- SPE is most consistent with D&J-predicted M_0 and M&M-predicted f_c

- Future work: New model

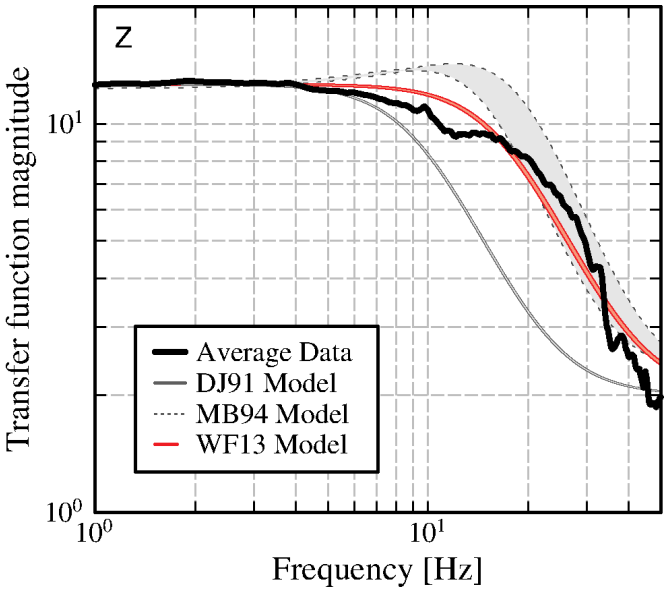

Moment tensor analysis of SPE-1 and -2

Sean Ford, Rob Mellors, and Bill Walter

SSA 2012

sean@llnl.gov

LLNL-PRES-552338

Calibration 1: Response

- H/V ratios of regional events similar between SN and TPNV
  - H/V noise ratio SN=5 TPNV=1¼ (much noisier horizontals)
- Long-period (15-25s) ratio of SN to TPNV teleseismic event provided ground-motion gain corrections
  - CMG-40T = 1, Trillium-120 = 1.5

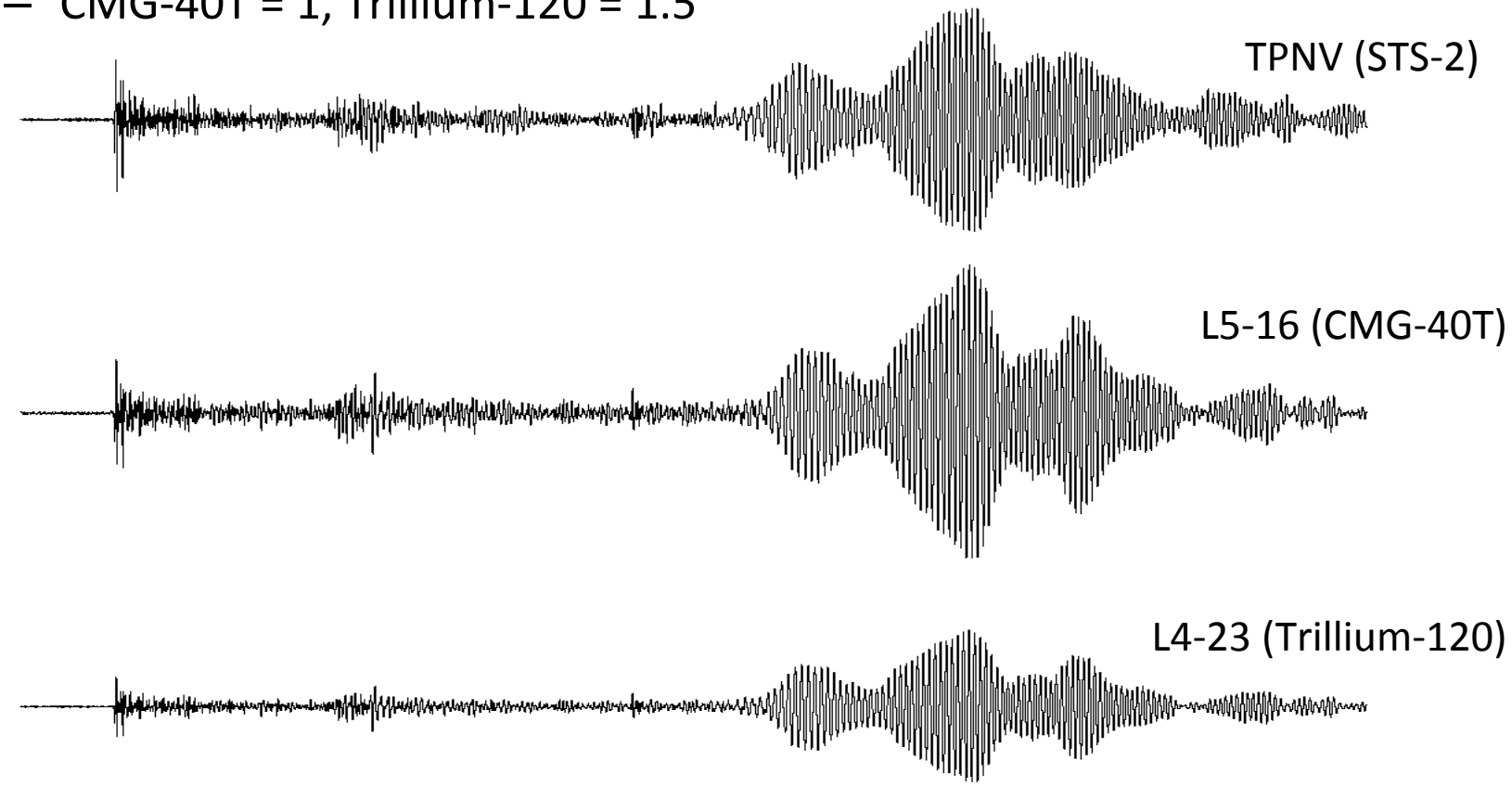

Calibration 2: Orientation

- Horizontal particle motion of teleseismic event
  - L1-20/L2-20/L3-20/L4-20/L5-16 = +5/0/?/0/-1

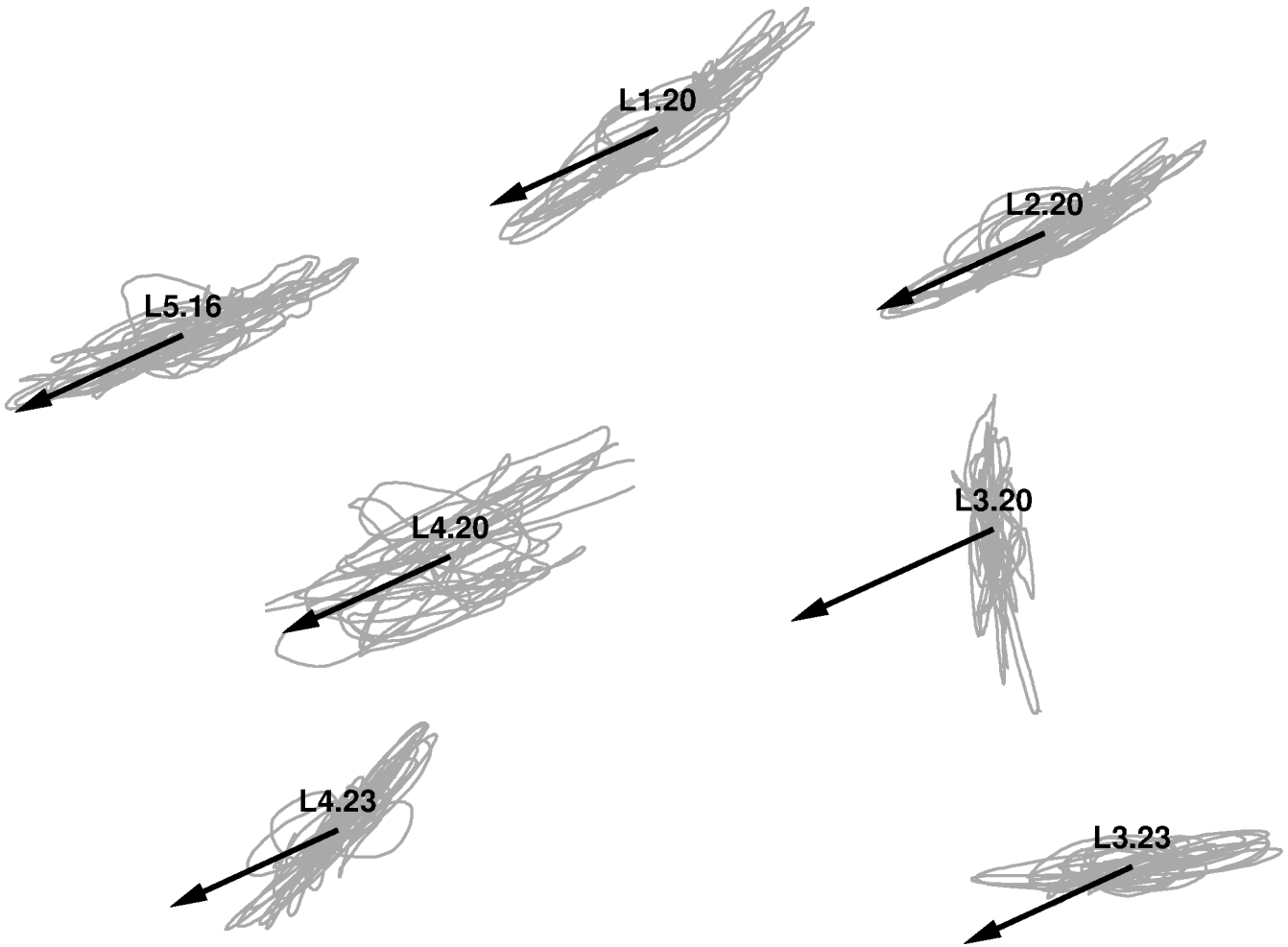

Data

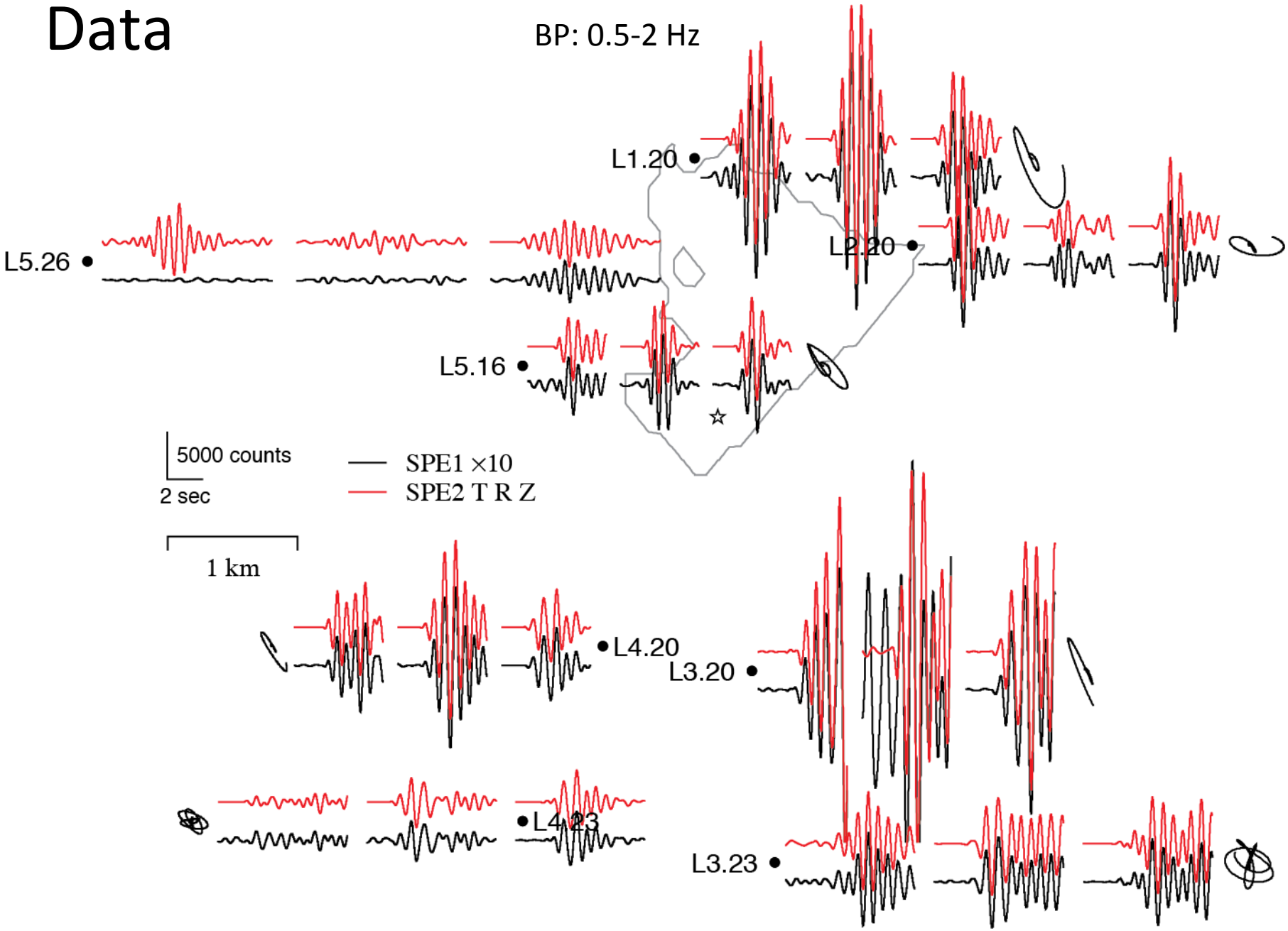
BP: 0.5-2 Hz
L1.20
L2.20
L5.26
L5.16
5000 counts
2 sec
SPE1 ×10
SPE2 T R Z
1 km
L4.20
L3.20
L4.23
L3.23

Velocity model

- V_P/V_S = 5000/2700 [m/s]
  - V_P/V_S = 1.852 v = 0.294
- 20m thick weathered layer
  - V_P/V_S = 2900/1600 [m/s]
- ρ = 2600/2650 kg/m^3
- Q = 600 / 300
- Constant to depth

Well log (Townsend et al., 2012)

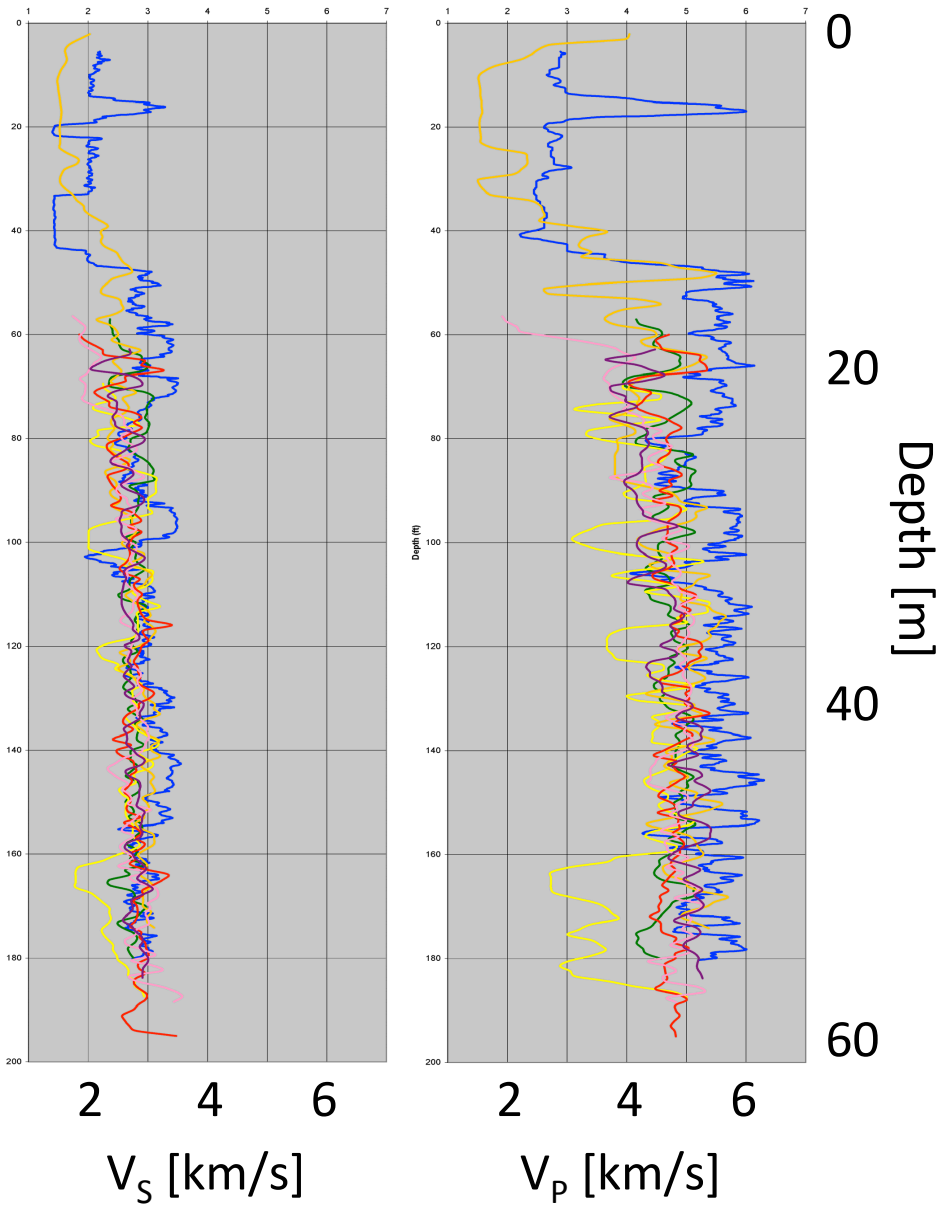

Data

3-component

Displacement

0.5 – 2 Hz

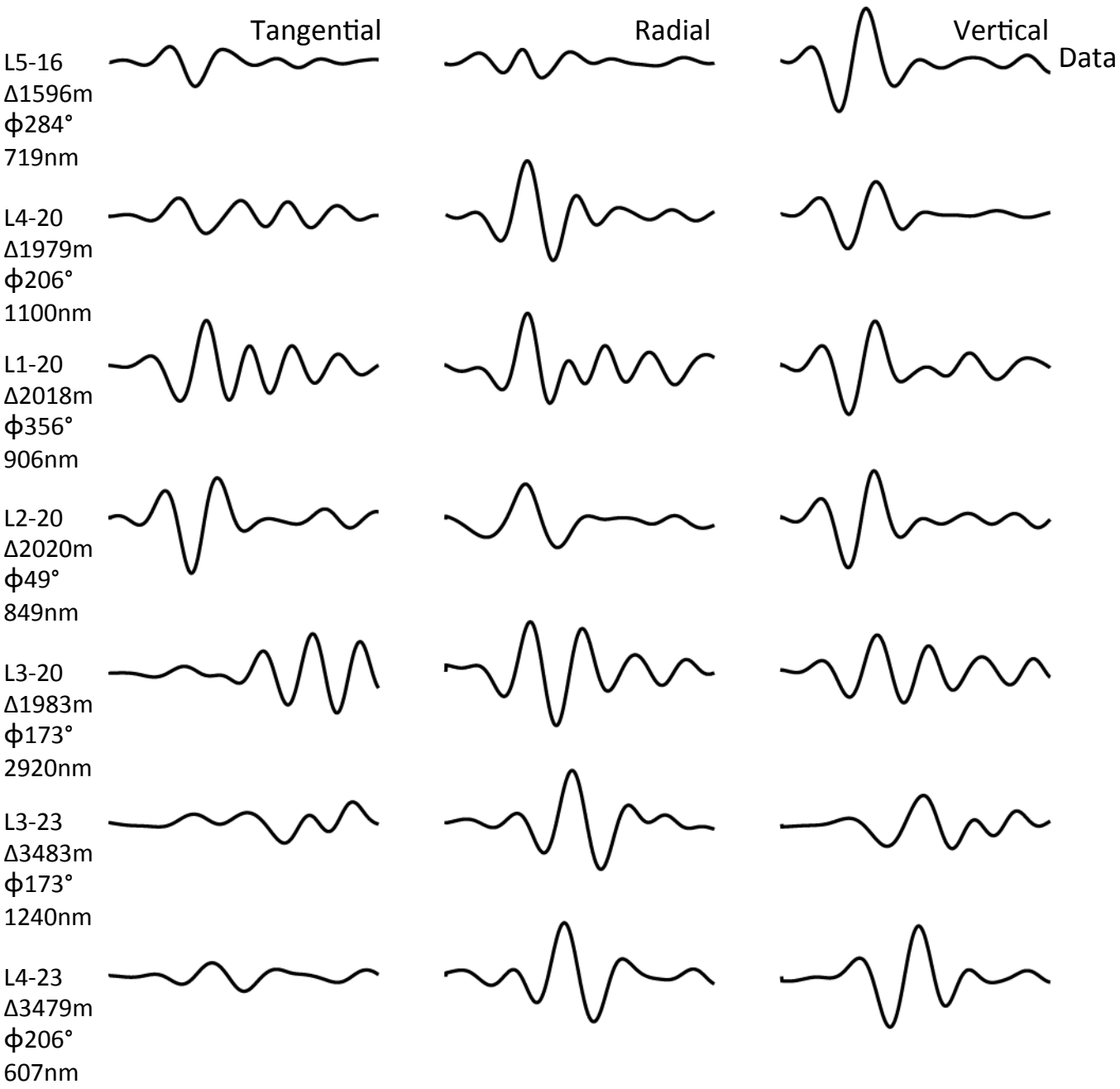

Explosion

$M_0 6.3 \times 10^{11}$ N-m

$M_W 1.8$

VR 44.5%

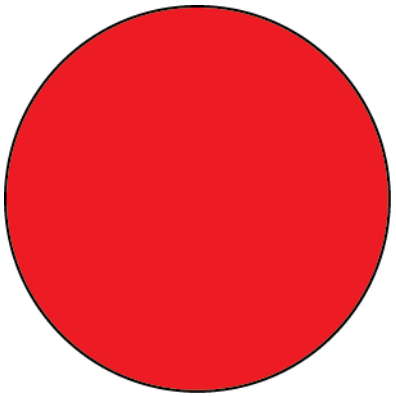

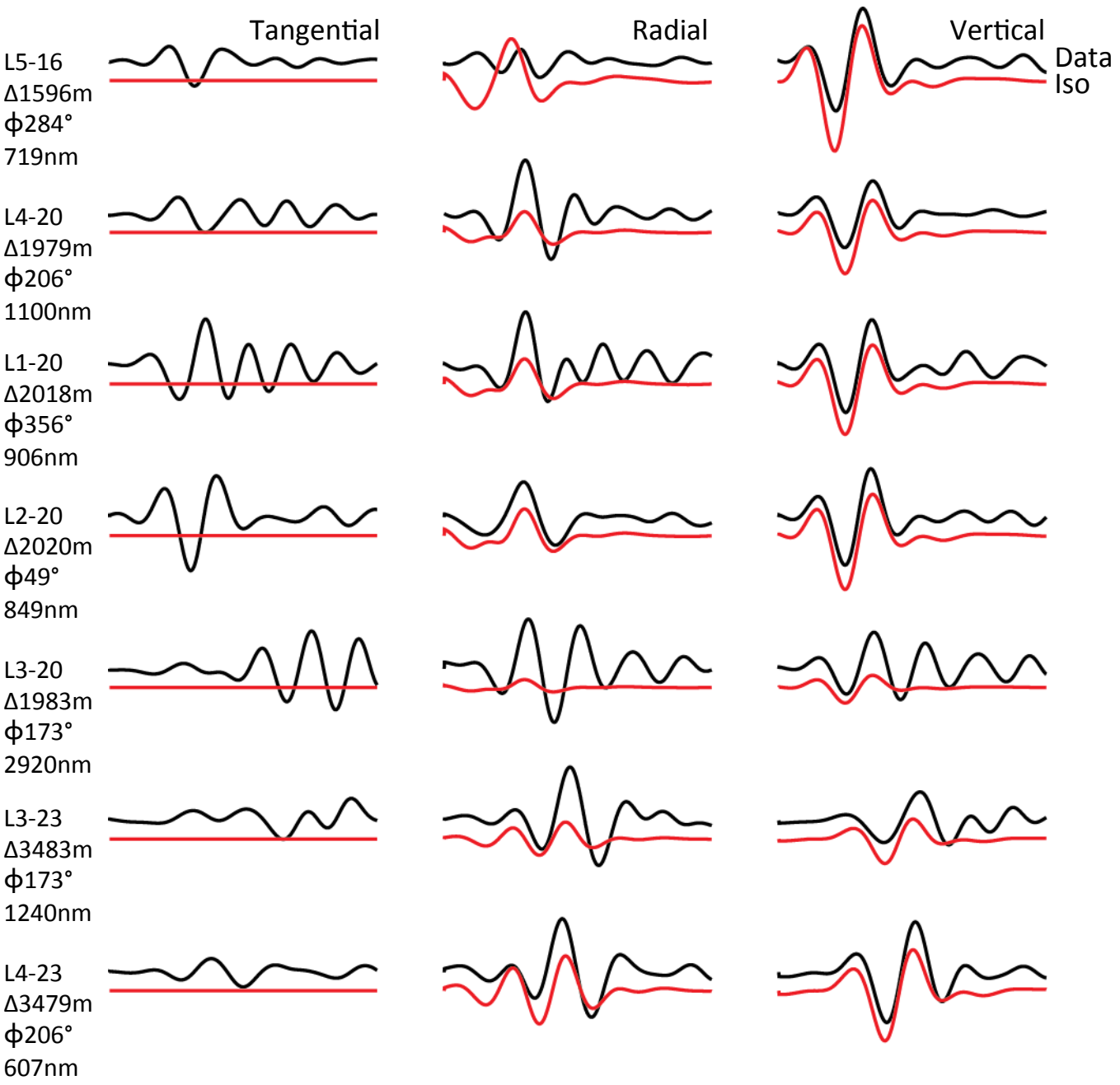

Full MT

$M_0$2.1×10^{12} N-m

M_W2.2

VR 48.4%

ISO/CLVD/DC

75 / 20 / 5

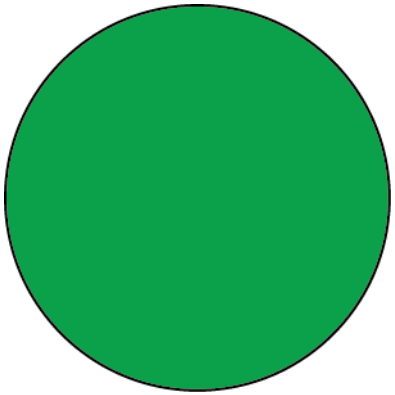

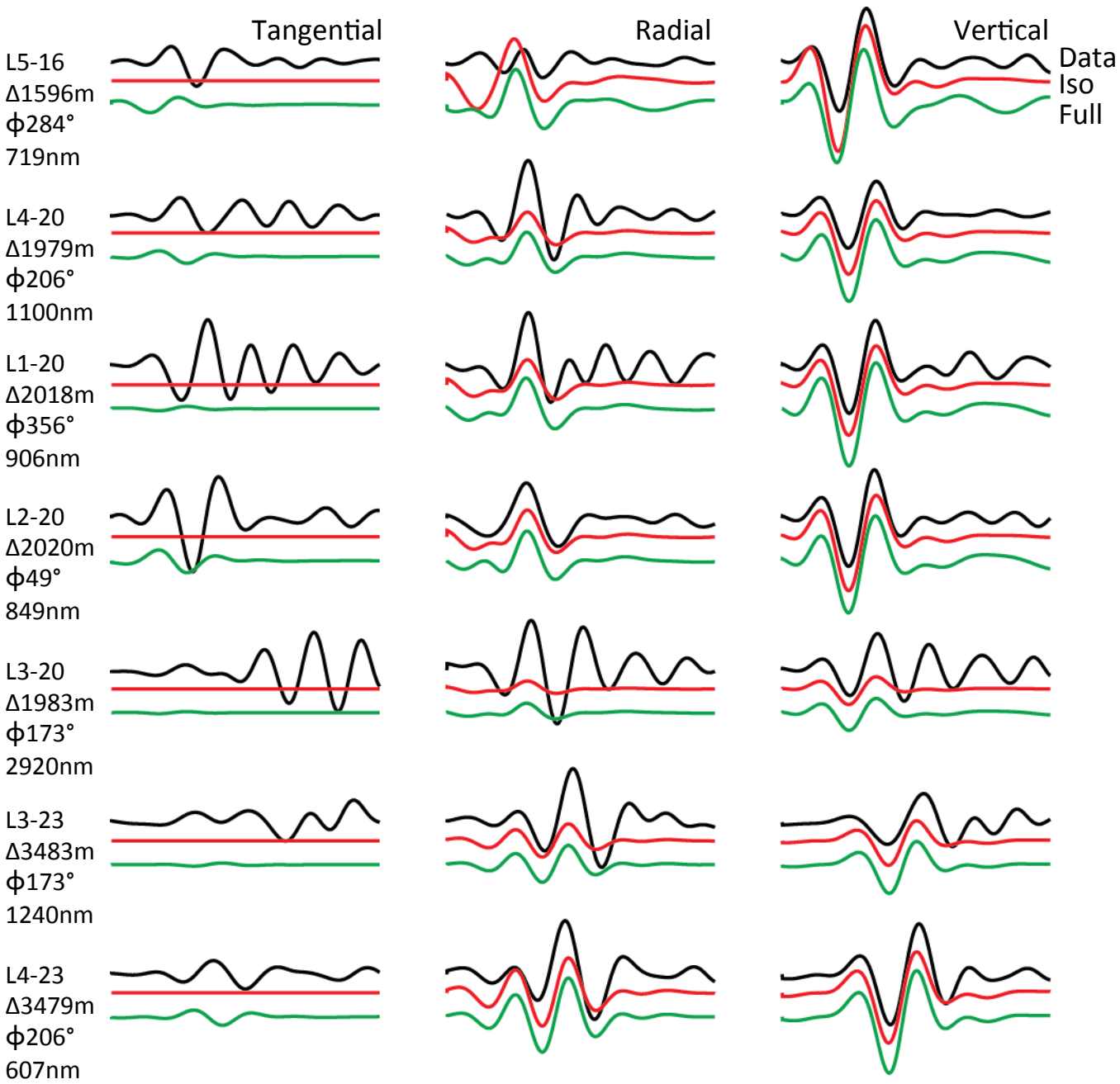

Deviatoric

$M_0 4.1 \times 10^{11}$ N-m

$M_W 1.7$

VR 42.3%

CLVD/DC

68 / 32

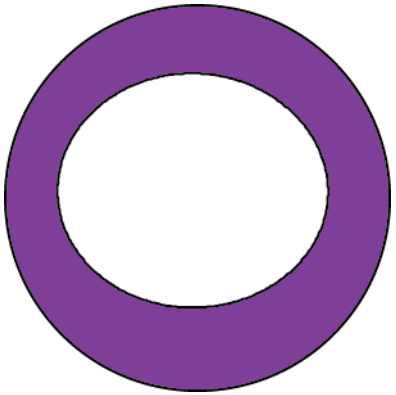

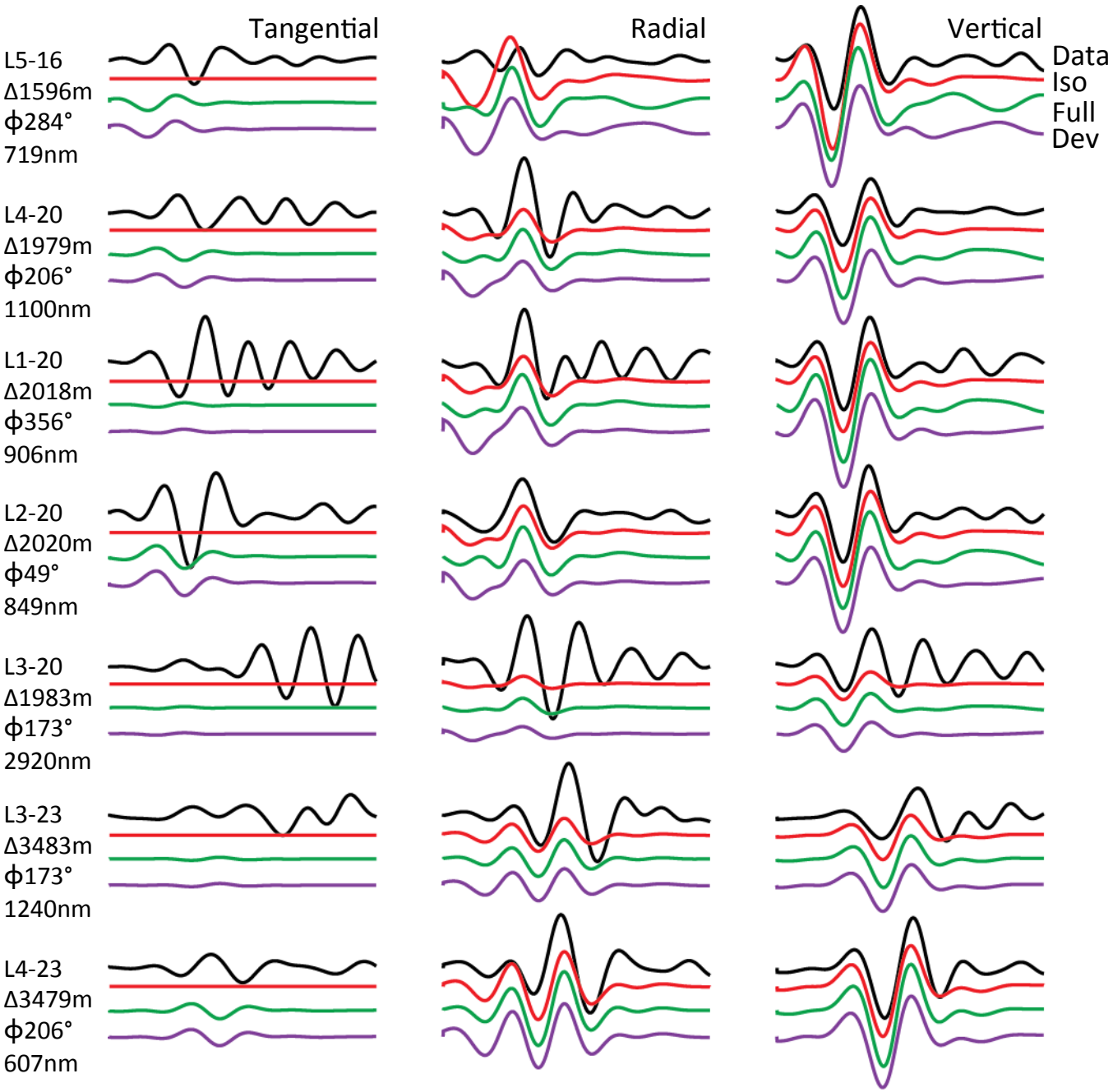

Best-DC

$M_0 3.1 \times 10^{11}$ N-m

$M_W 1.6$

VR 36.7%

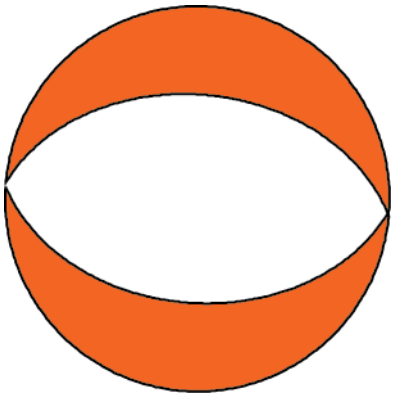

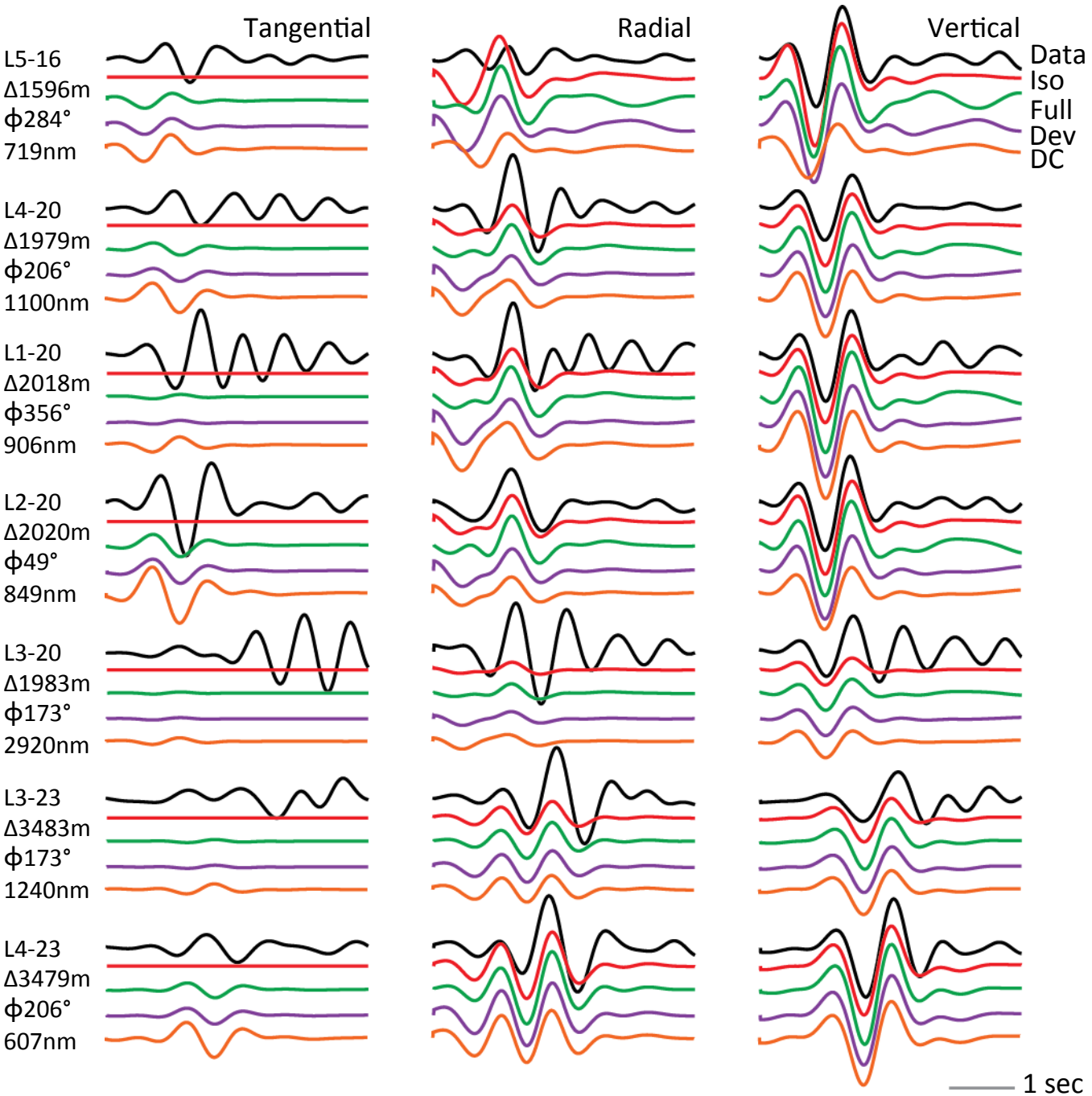

Explosion

$M_0 10.9 \times 10^{11}$ N-m

$M_W 1.9$

60%

+ DC

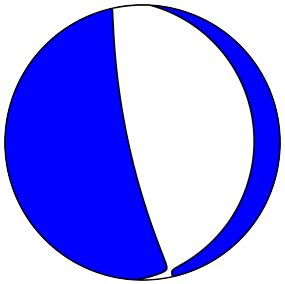

$M_0 8.6 \times 10^{11}$ N-m

$M_W 1.7$

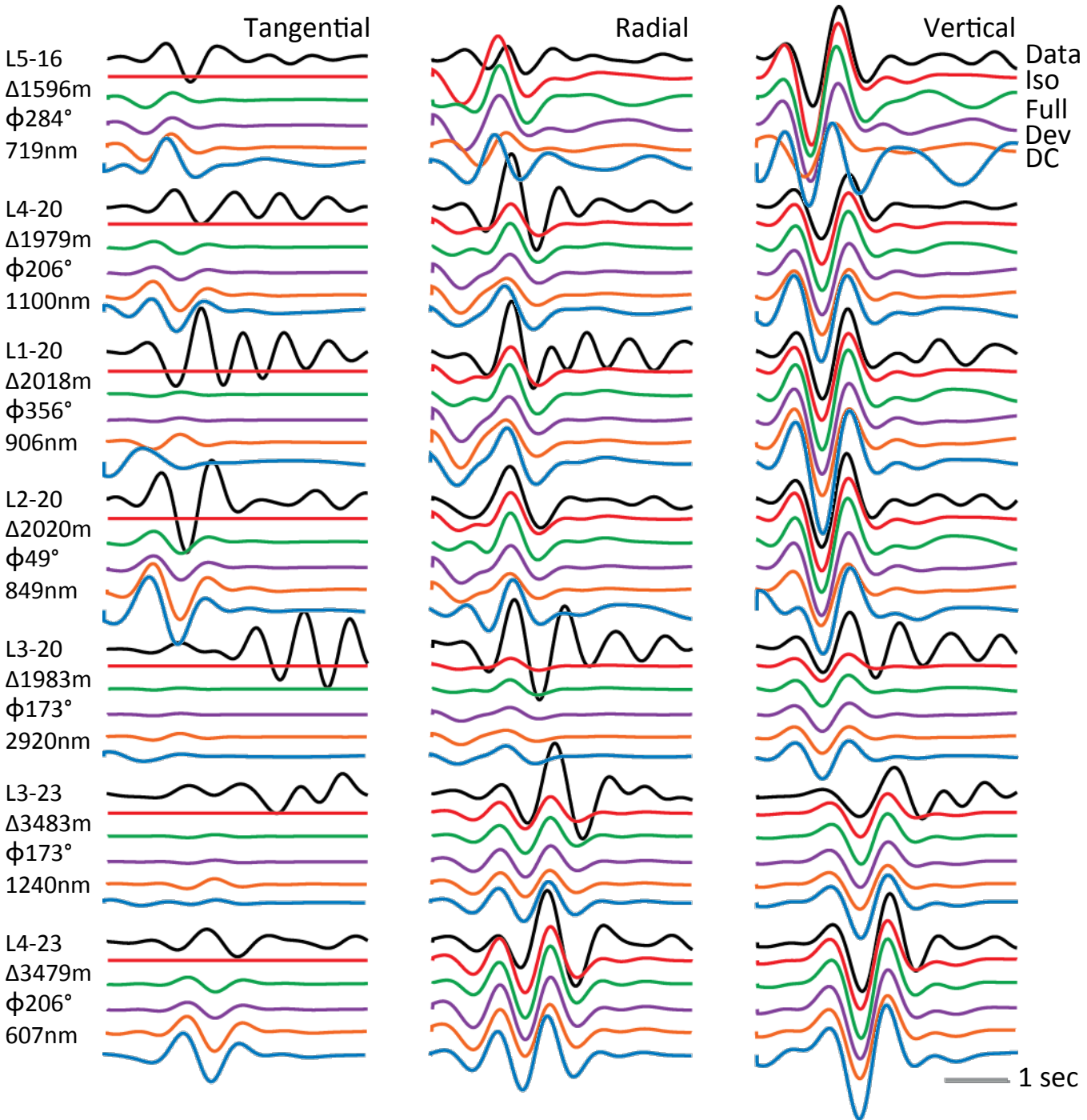

Explosion

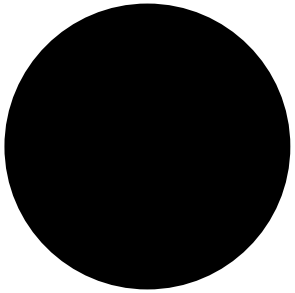

1D GFs

M_0 63×10^{10} N-m

3D GFs

M_0 38×10^{10} N-m

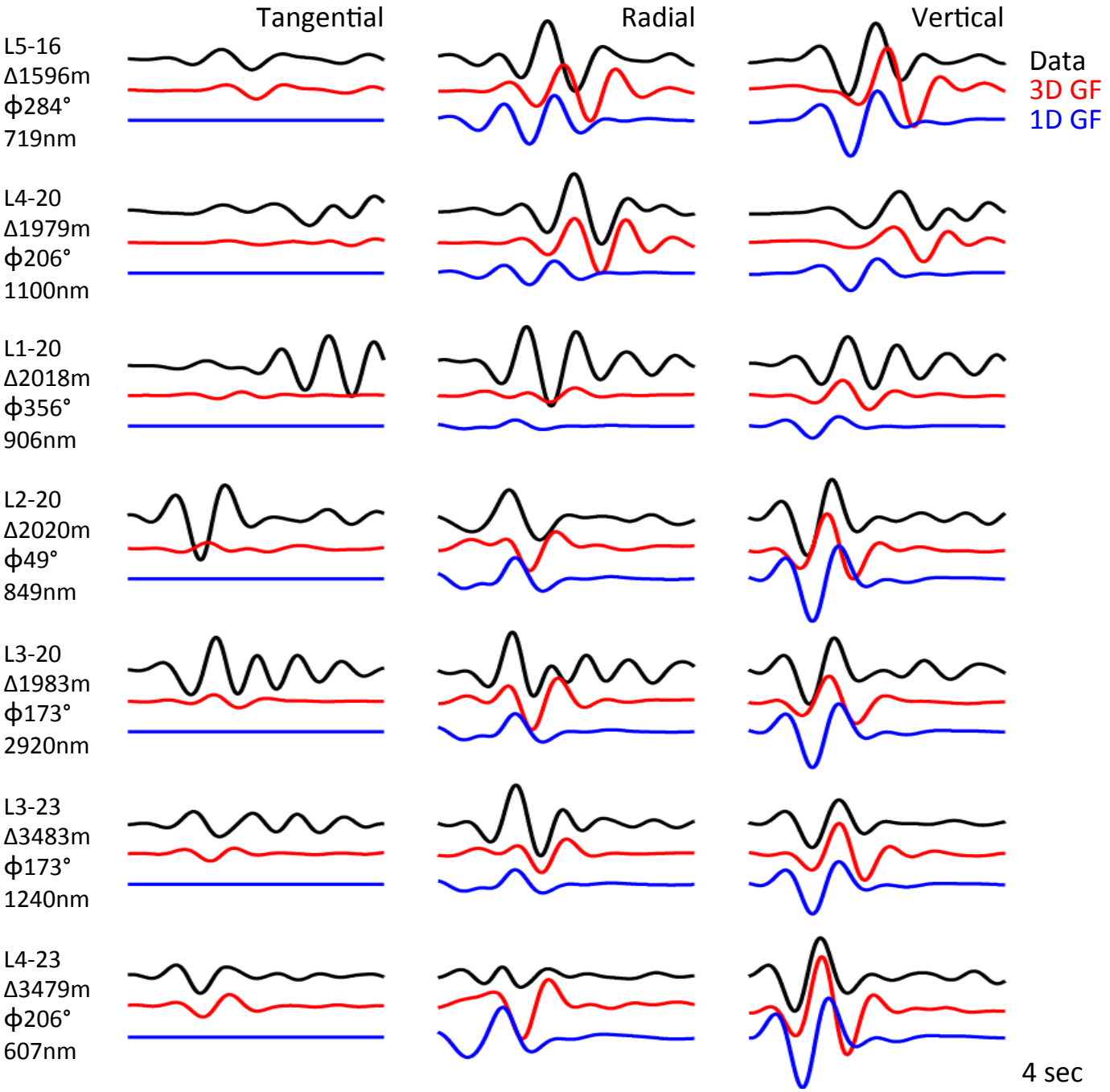

Source-type plot (Hudson et al., 1989)

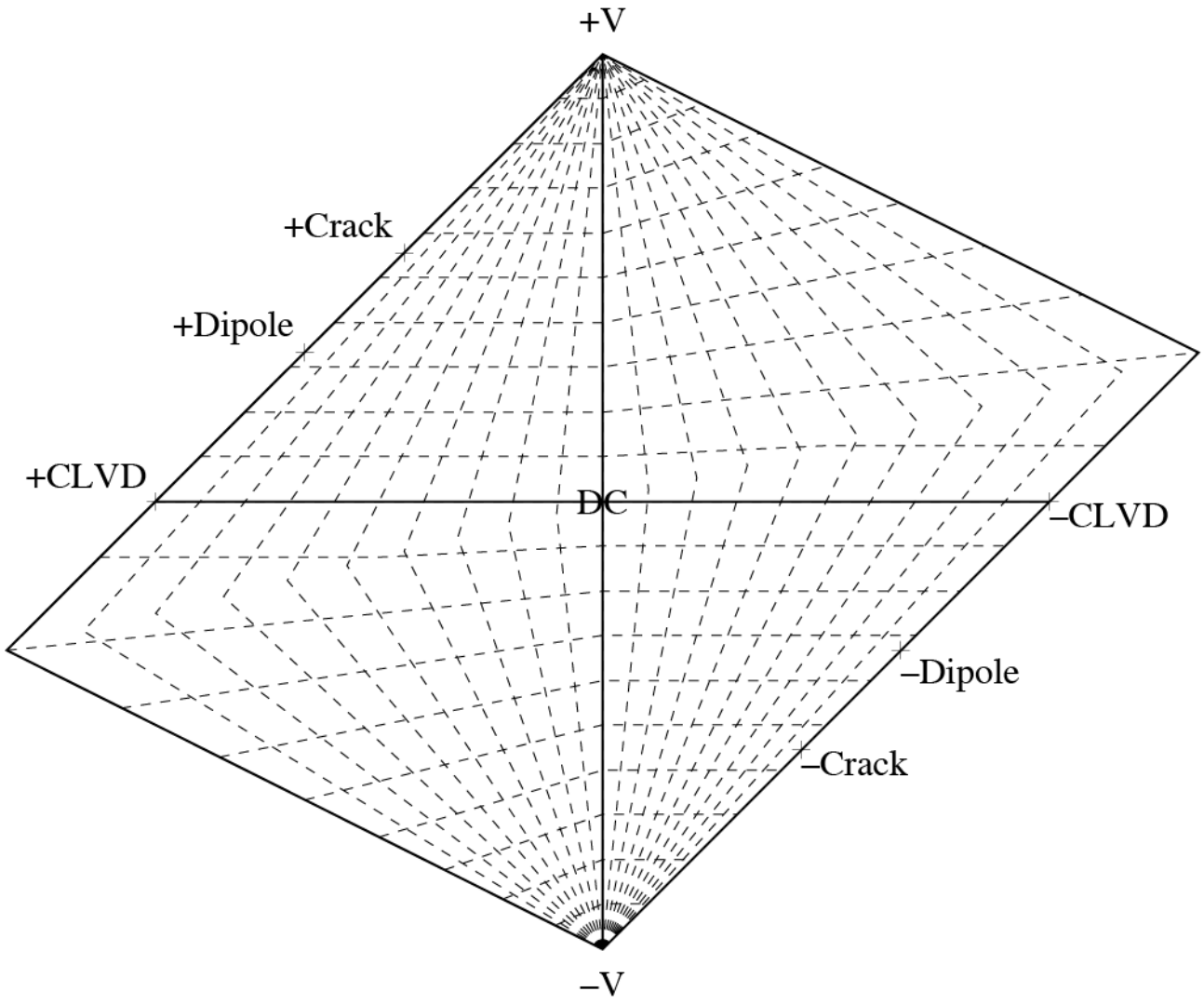

Source-type plot (Hudson et al., 1989)

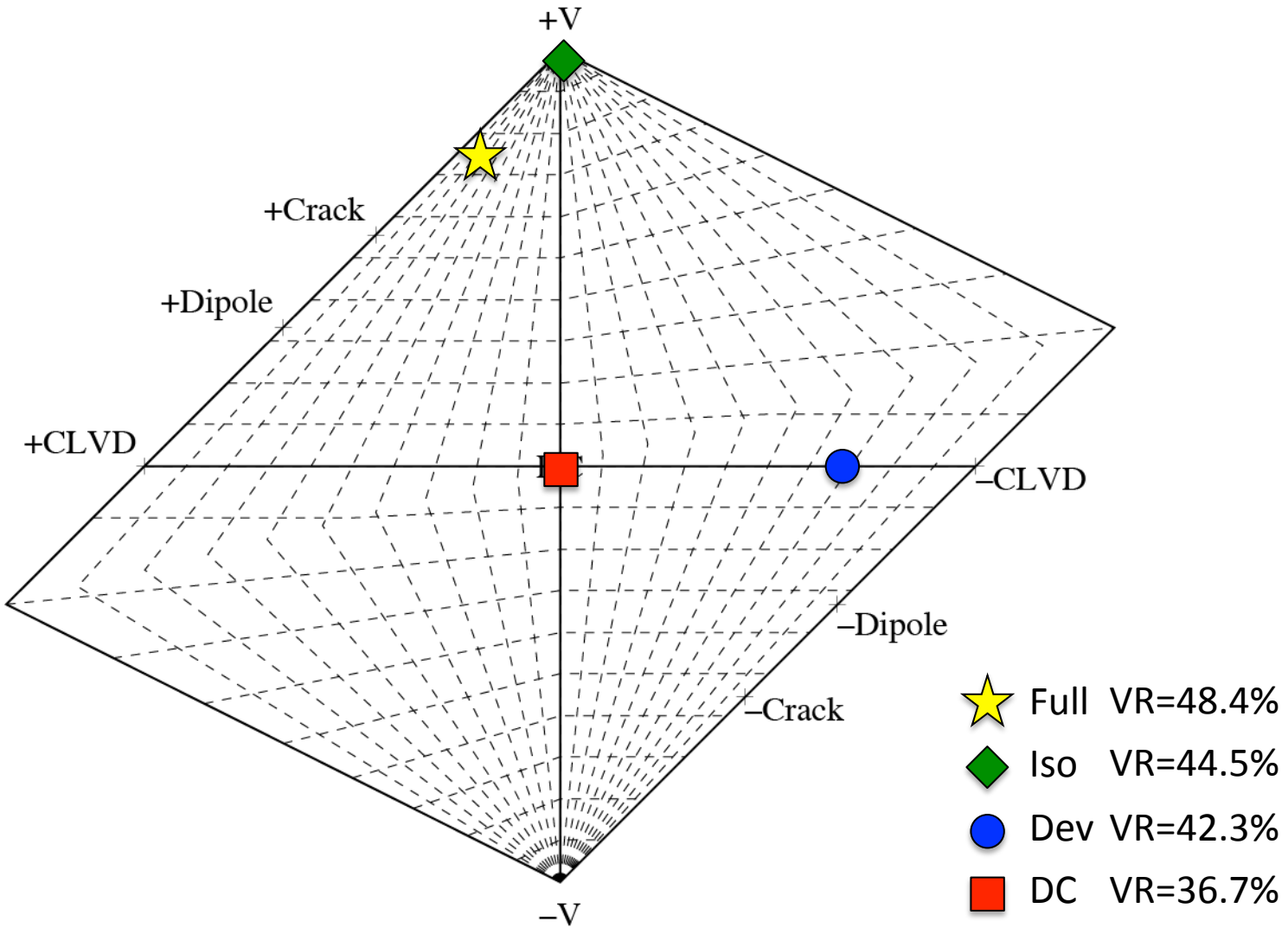

SPE-1

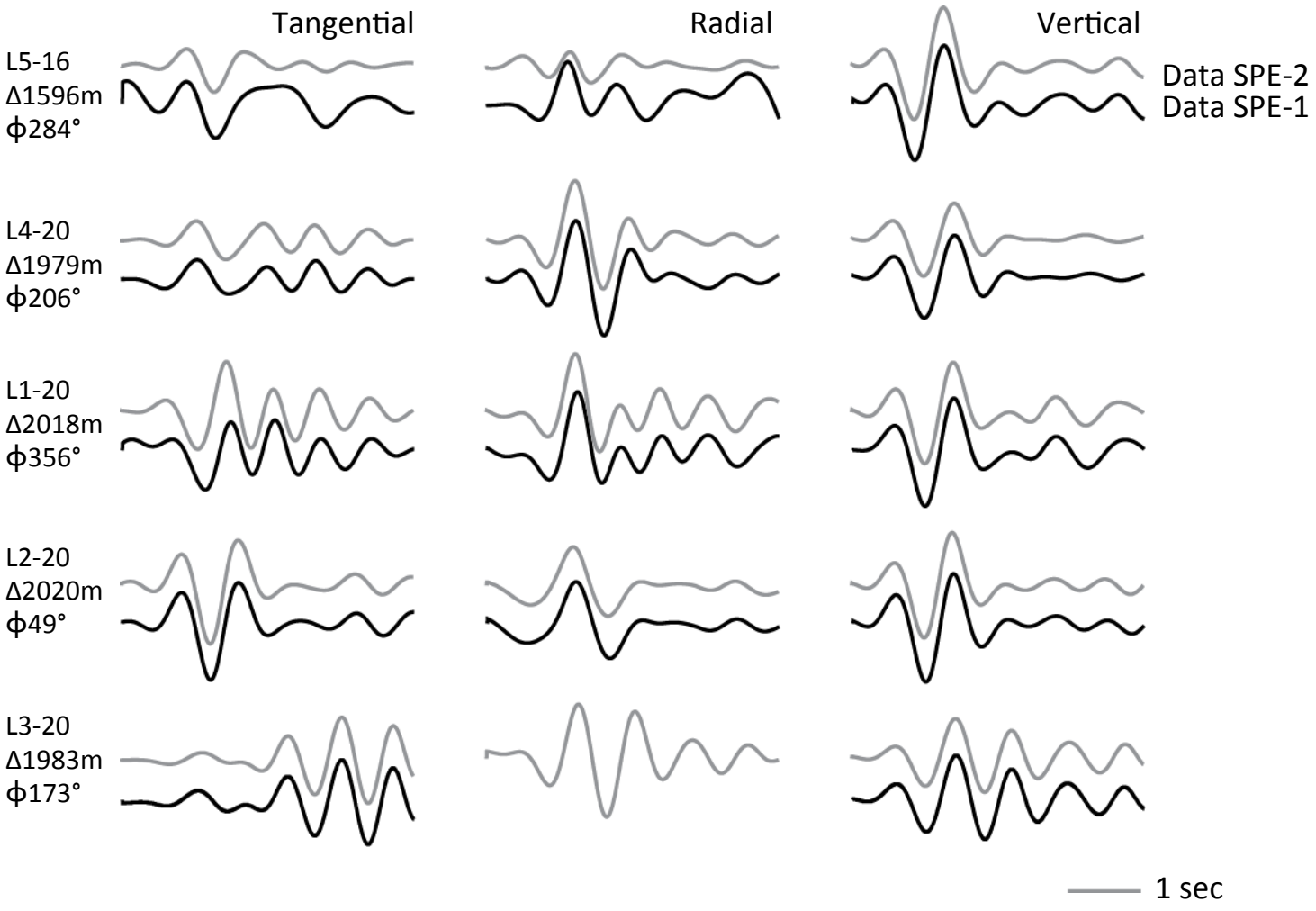
Tangential
Radial
Vertical
Data SPE-2
Data SPE-1
L5-16
Δ1596m
ϕ284°
L4-20
Δ1979m
ϕ206°
L1-20
Δ2018m
ϕ356°
L2-20
Δ2020m
ϕ49°
L3-20
Δ1983m
ϕ173°
1 sec

SPE-1 Explosion - 6×10^{10} N-m (M_W1.2)

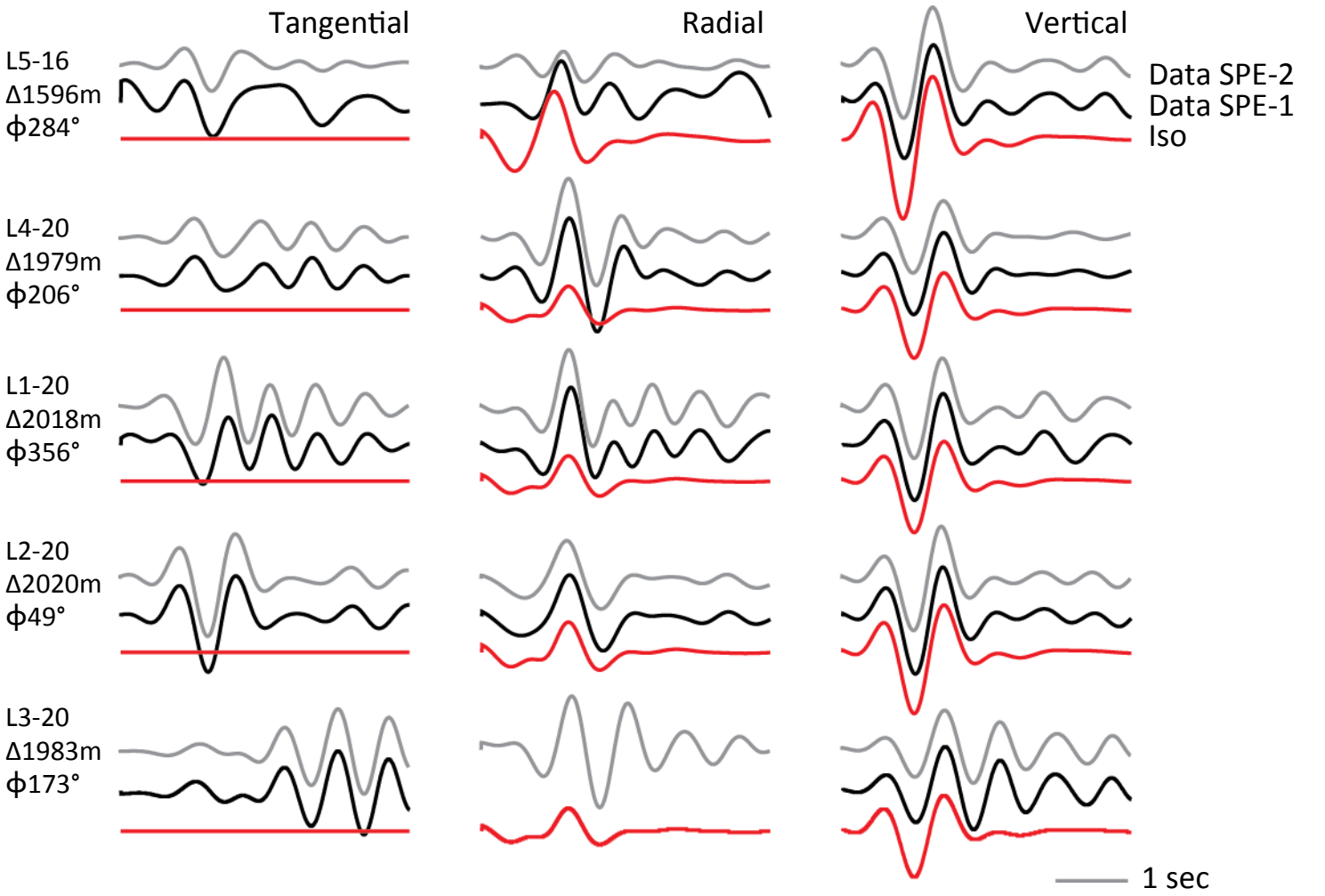

- M_0(SPE-2) ≅ 10 × M_0(SPE-1)

Deconvolution for relative moment-rate

- Deconvolve SPE-1 from SPE-2 on L5-16 vertical at <40 Hz

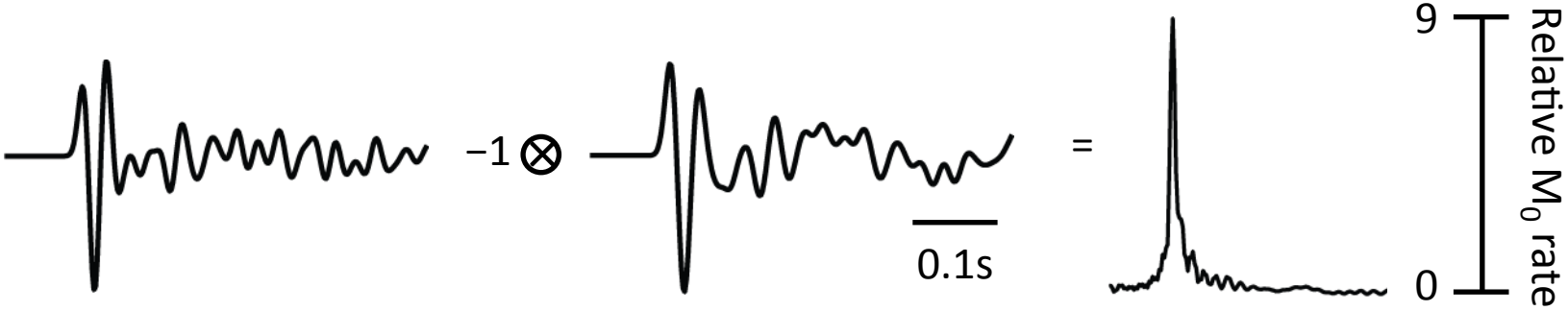

Deconvolution for relative moment-rate

- Deconvolve SPE-1 from SPE-2 on L5-16 vertical at <40 Hz

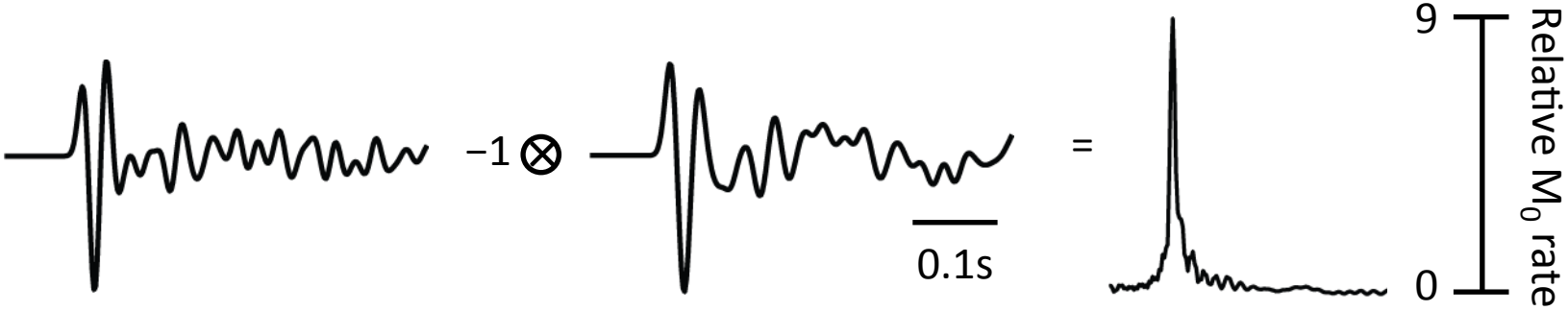

- Convolve moment-rate function with SPE-1 L5-16 all channels

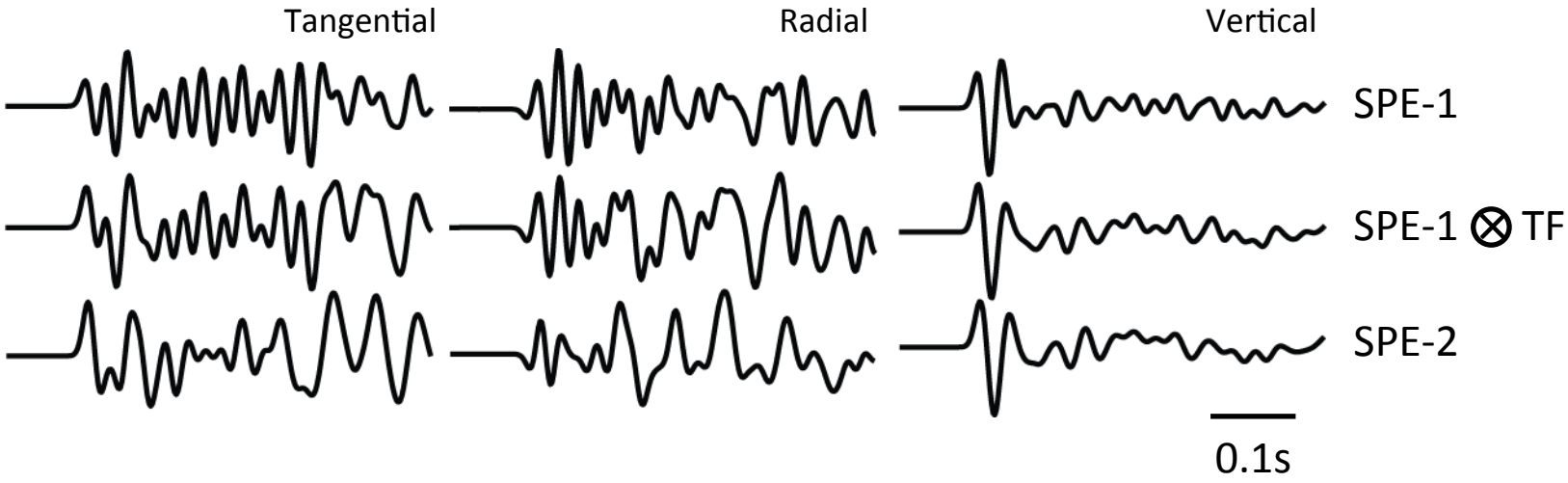

Denny & Johnson (1991) scaling relations

- Regression for cavity radius as a function of yield obtained

$$R_c = \frac{1.47 \times 10^4 W^{1/3}}{\beta^{0.3848} P_0^{0.2625} 10^{0.0025 GP}}$$

- Regression for seismic moment obtained

$$M_0 = \frac{1}{311} M_t P_0^{0.349} 10^{-0.027 GP} \qquad \text{where} \qquad M_t = \frac{4}{3} \pi \rho \alpha^2 R_c^3$$

- Prediction of R_c for SPE-1/-2 = 0.79 / 1.79 m

- Explosion M_0 predicts W for SPE-1/2 = 98 / 945 kg TNT

Preliminary findings

- SPE-2 best-fit isotropic M_0 6.3×10^{11} N-m = 10 × SPE-1 isotropic M_0
- SPE-1/-2 low-frequency waveforms are very similar
- Full MT low-frequency point-source inversion cannot fit tangential displacement
- Evidence for multipathing requires >1D velocity-model

Future work

- Distributed source
- Variable 1D models to capture M_0 error
- Higher frequency and greater bandwidth inversions
- Variable weighting of low-amplitude initial arrivals
- Use of eGF for kinematic source inversion

Coda wave interferometry of SPE-2/-3 for velocity change due to damage

Sean Ford, LLNL

Approach

- GS11D-vertical observations of SPE-2/-3
- Non-overlapping windows of 0.4 s ($10 \times T_{dom}$)
- Damage should change elastic properties leading to velocity change and travel-time perturbation
- Use coda wave interferometry to measure travel-time perturbation [Snieder et al., 2002]

$$\frac{\delta v}{v} = -\frac{\delta t}{t}$$

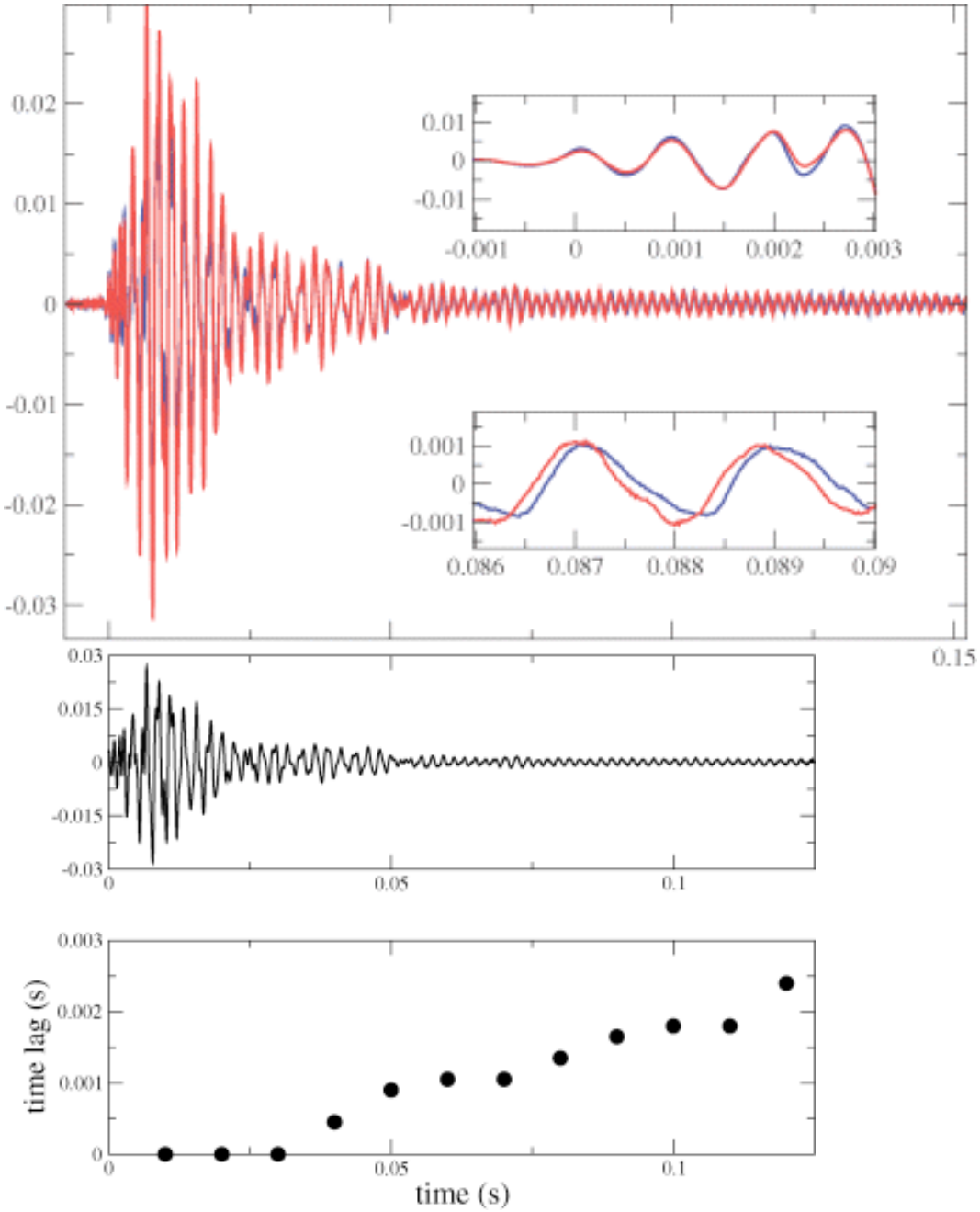

Example from Gret et al. [2006] *Geophys. J. Int.*

Two waveforms, one measured at 4.14 MPa of pressure in the cell (blue) and one measured at 12.41 MPa (red). The upper panel shows the early time window and the lower panel part of the coda.

The seismic record (top panel), and estimates of δt for multiple time-windows (bottom panel). The first three points are computed from the early part of the waveform and are not sufficiently sensitive to detect the velocity change.

Analysis at L4-05 (Δ=500m)

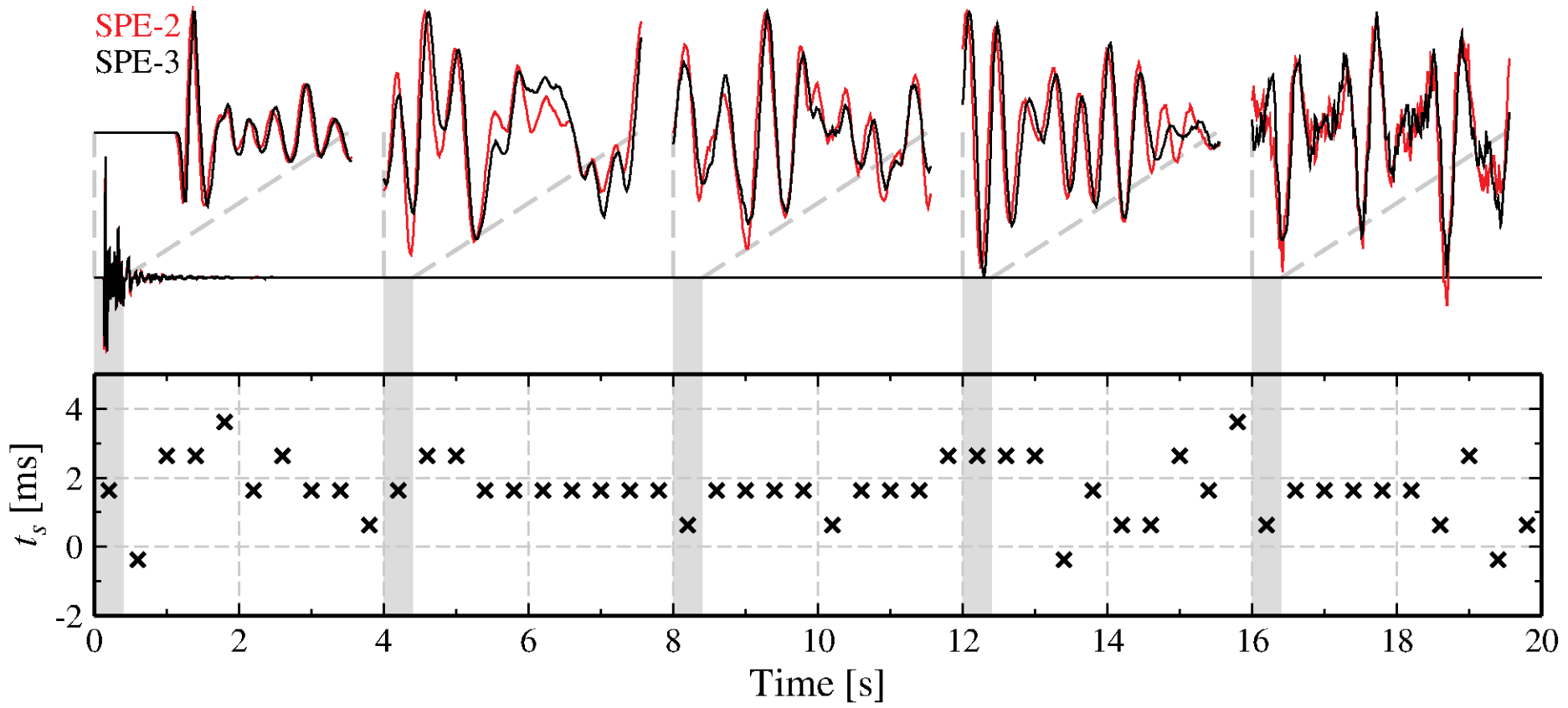

Analysis at all stations

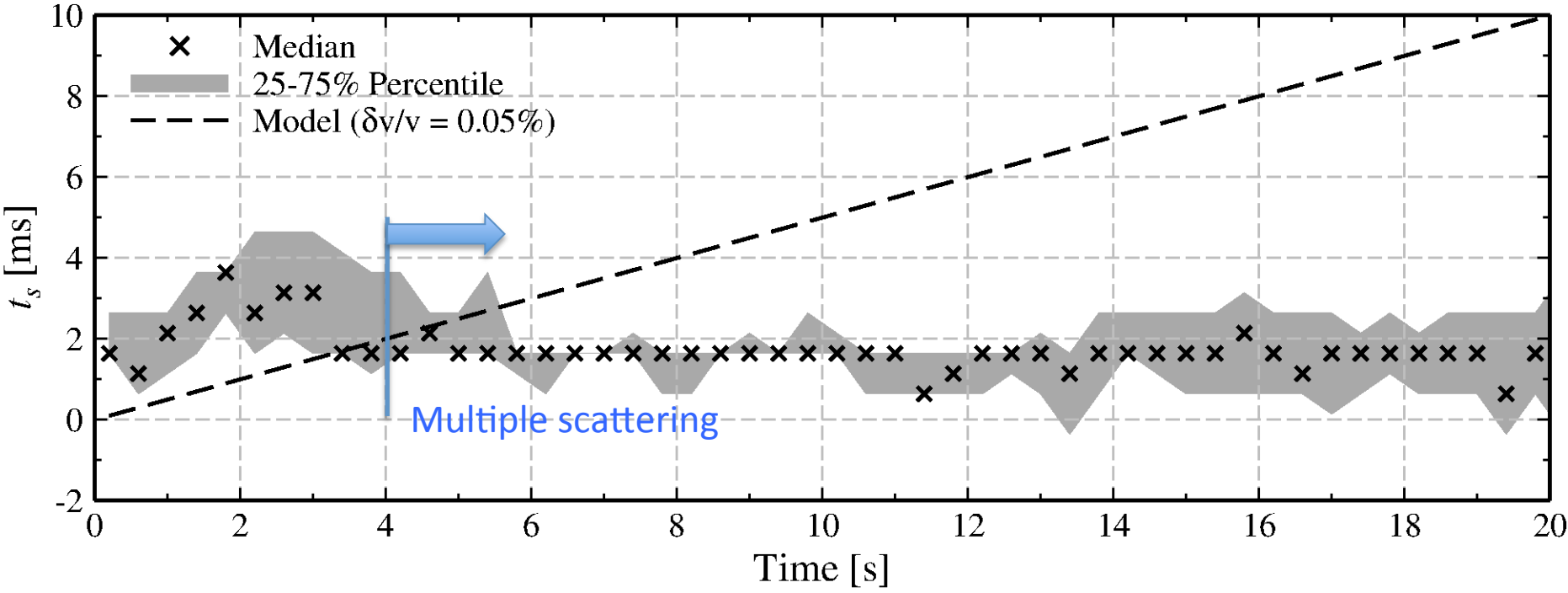

Prediction

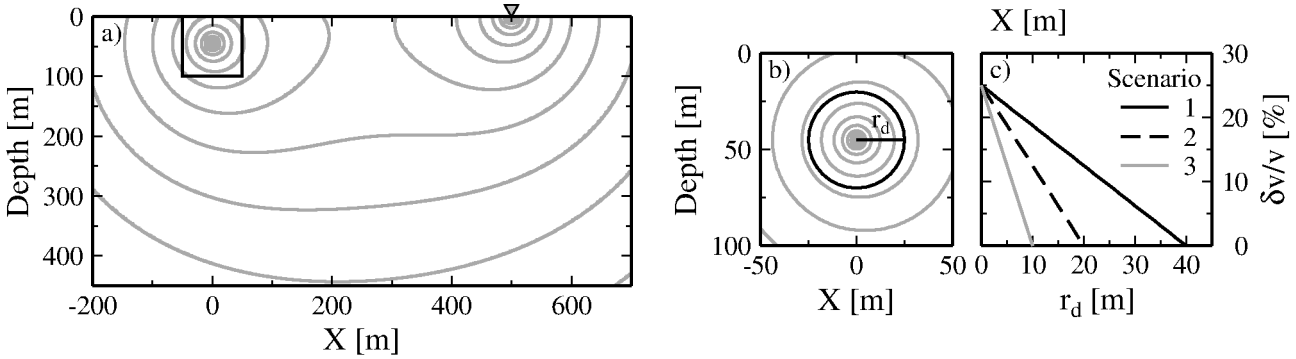
a)
Depth [m]
X [m]
b)
Depth [m]
X [m]
c)
Scenario
1
2
3
δv/v [%]
r_d [m]

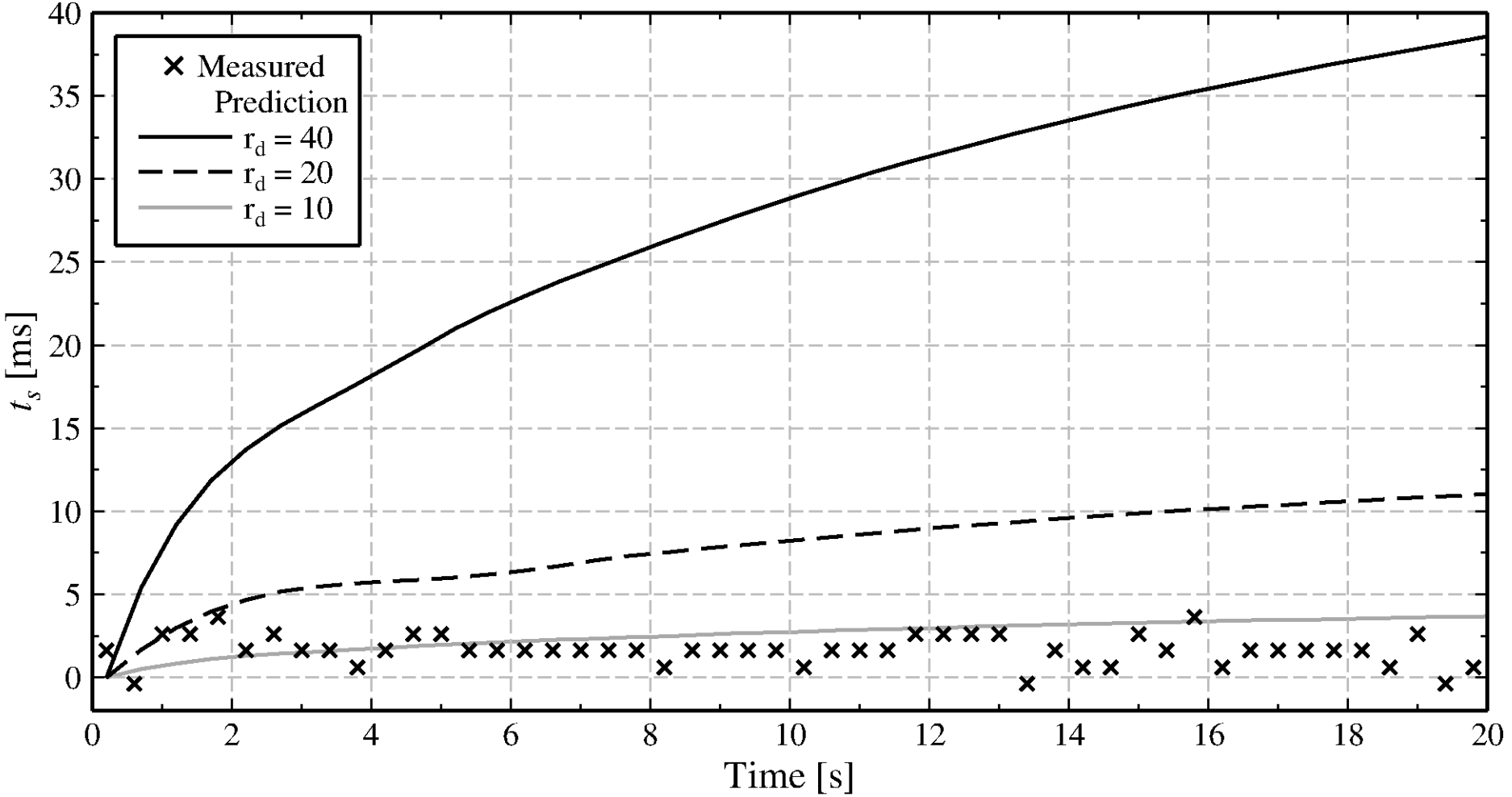
Measured
Prediction
r_d = 40
r_d = 20
r_d = 10
t_s [ms]
Time [s]

Near-field data

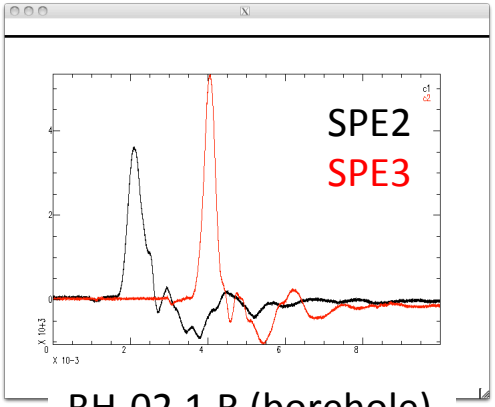

BH-02.1.R (borehole)

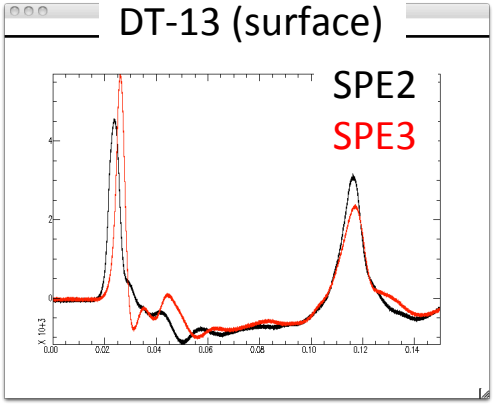

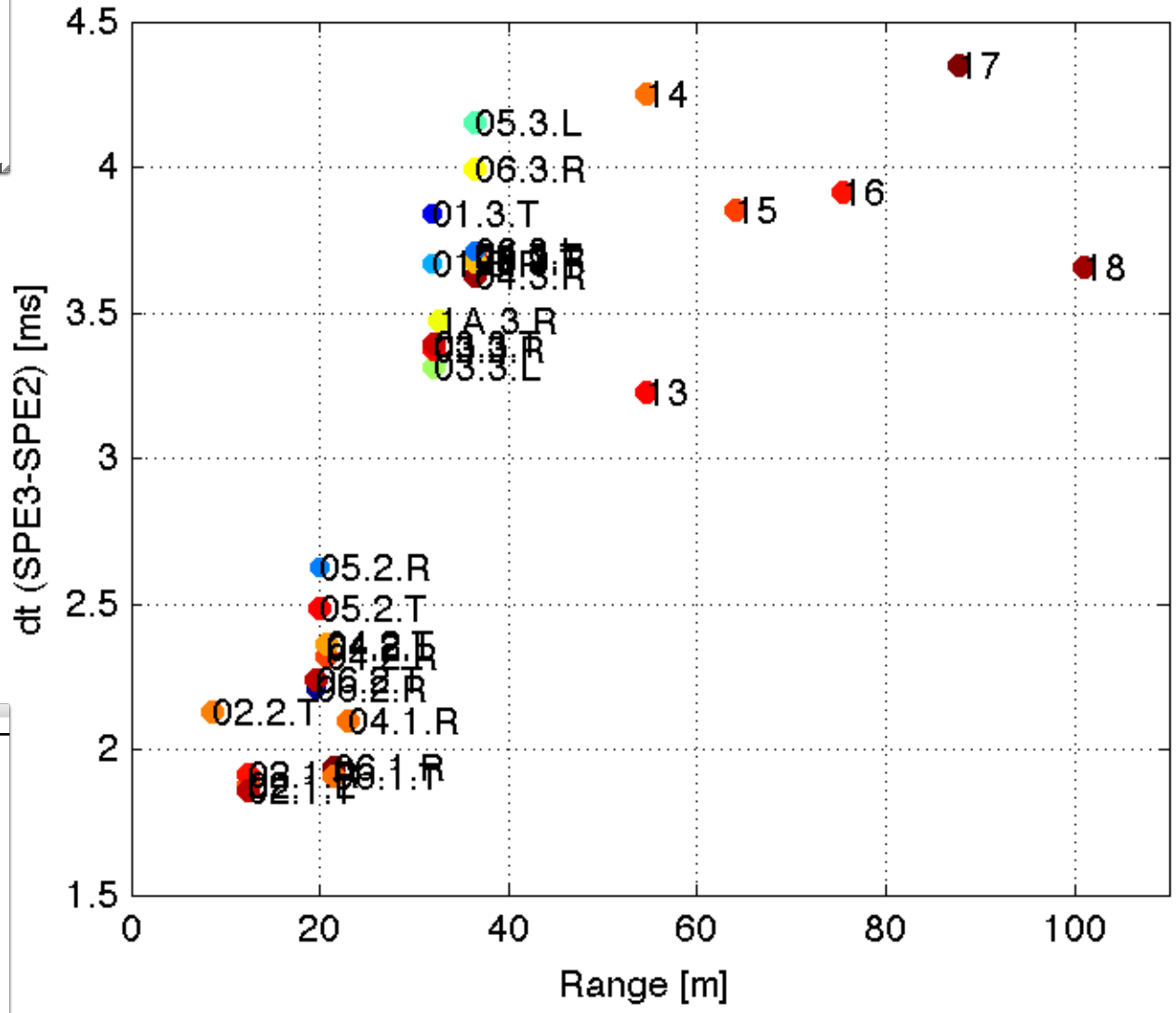

1D inversion for slowness perturbation

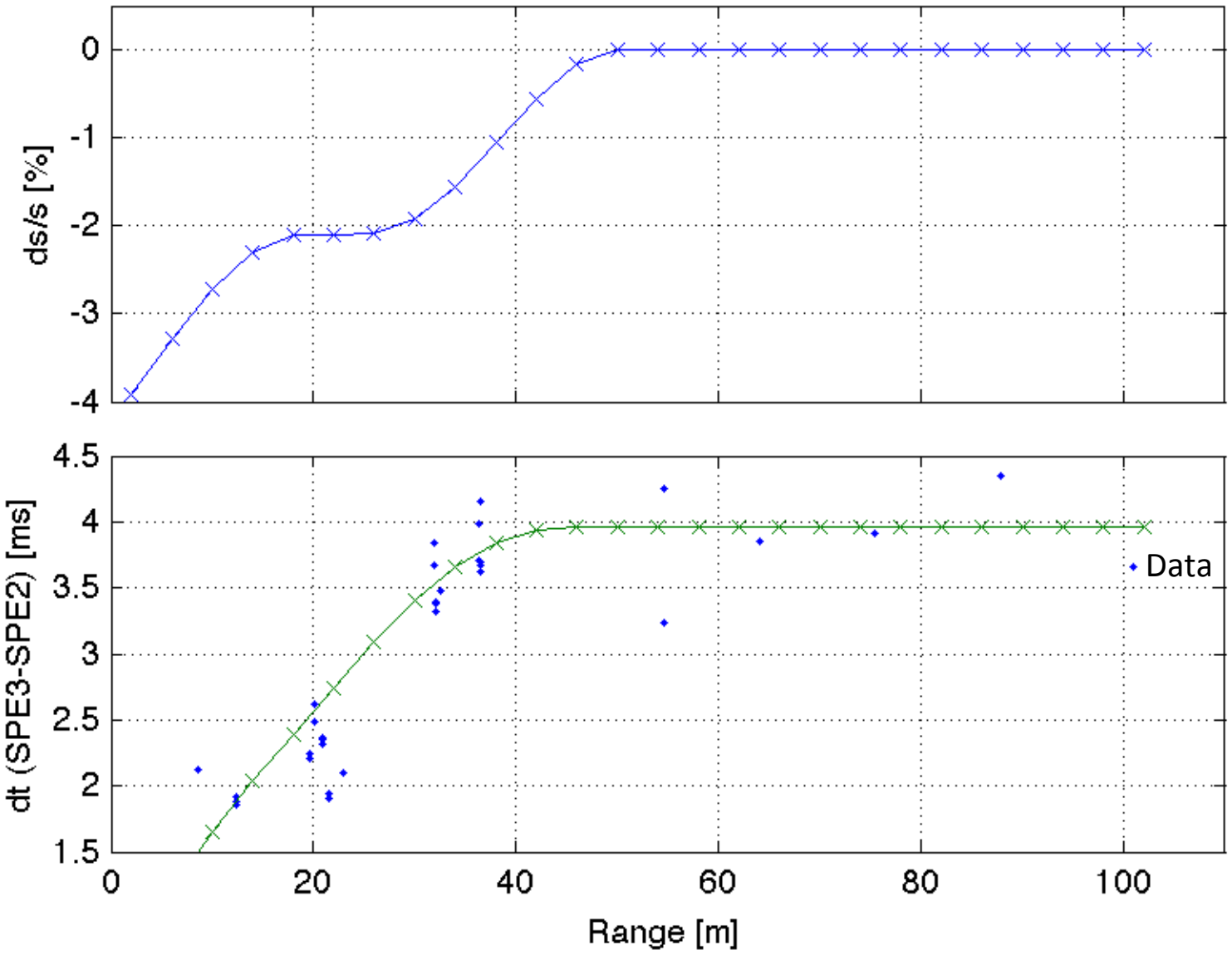

1D inversion for slowness perturbation

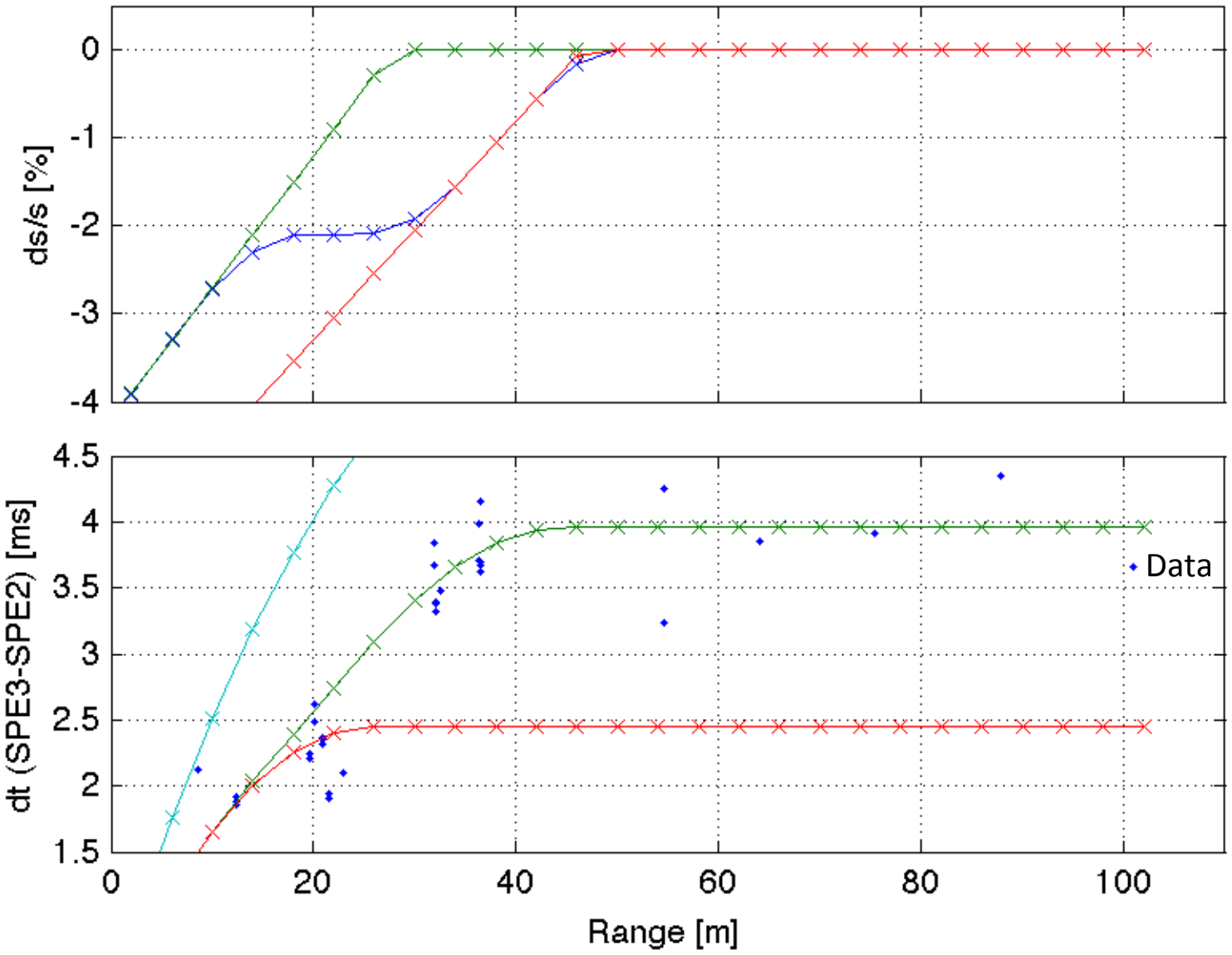

To Do

- Note SPE W and h
- Note historical parameters

A Spall Model Comparison with Insights from the Source Physics Experiment

Sean Ford and Rob Mellors, LLNL

Lawrence Livermore National Laboratory is operated by Lawrence Livermore National Security, LLC, for the U.S. Department of Energy, National Nuclear Security Administration under Contract DE-AC52-07NA27344.

Spall model

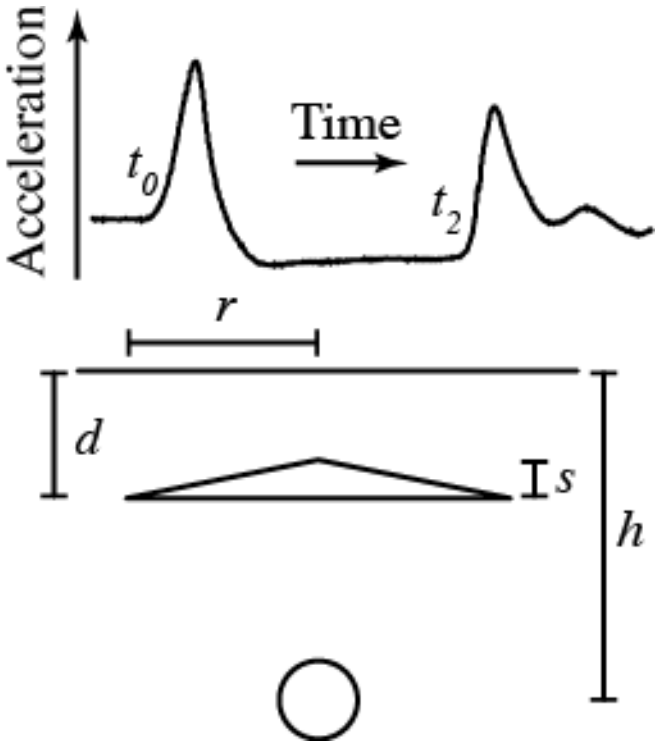

Study	Depth (d) [m]	Lateral extent (r) [m]	Maximum gap (s) [m]	Peak velocity (v) [m/s]
Viecelli (1973)	$10^{3.44}\ W^{2/3}h^{-1}$	$100\ W^{1/3}$	$10^{8.82}\ W^{4/3}h^{-4}$	from s via eq (2)
Sobel (1978)	$22\ W^{1/3}$	$10^{2.84}\ W^{0.37}h^{-0.16}$	$10^{0.57}\ W^{0.52}h^{-0.50}$	from s via eq (2)
Patton (1990)*	$54\ W^{0.25}$	$334\ W^{0.25}$	from v via eq (1)	$10^{4}\ W^{1.61/3}\ h^{-1.61}$

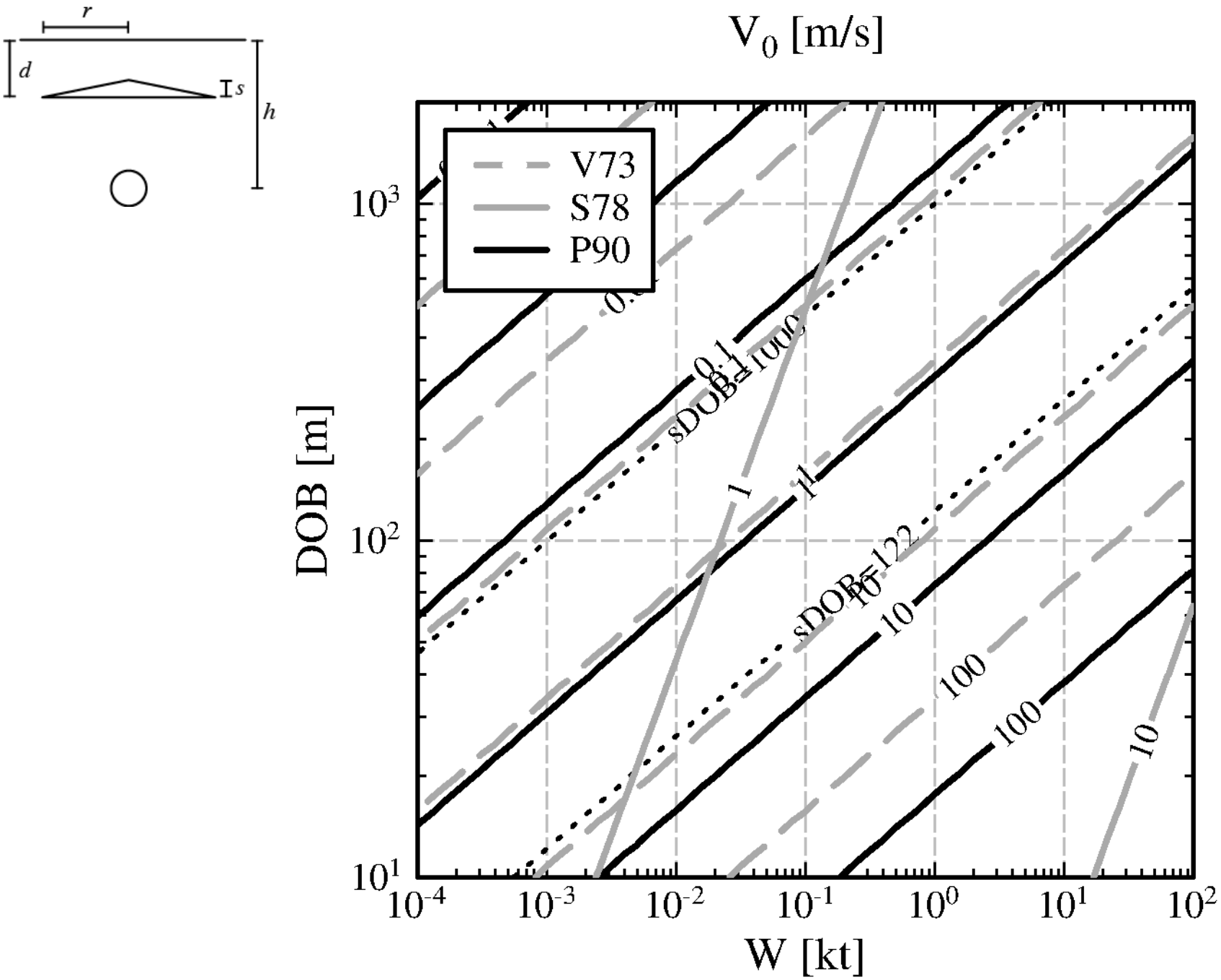
r
d
Is
h
V0 [m/s]
V73
S78
P90
sDOB=100
sDOB=122
DOB [m]
W [kt]
10^3
10^2
10^1
10^-4
10^-3
10^-2
10^-1
10^0
10^1
10^2

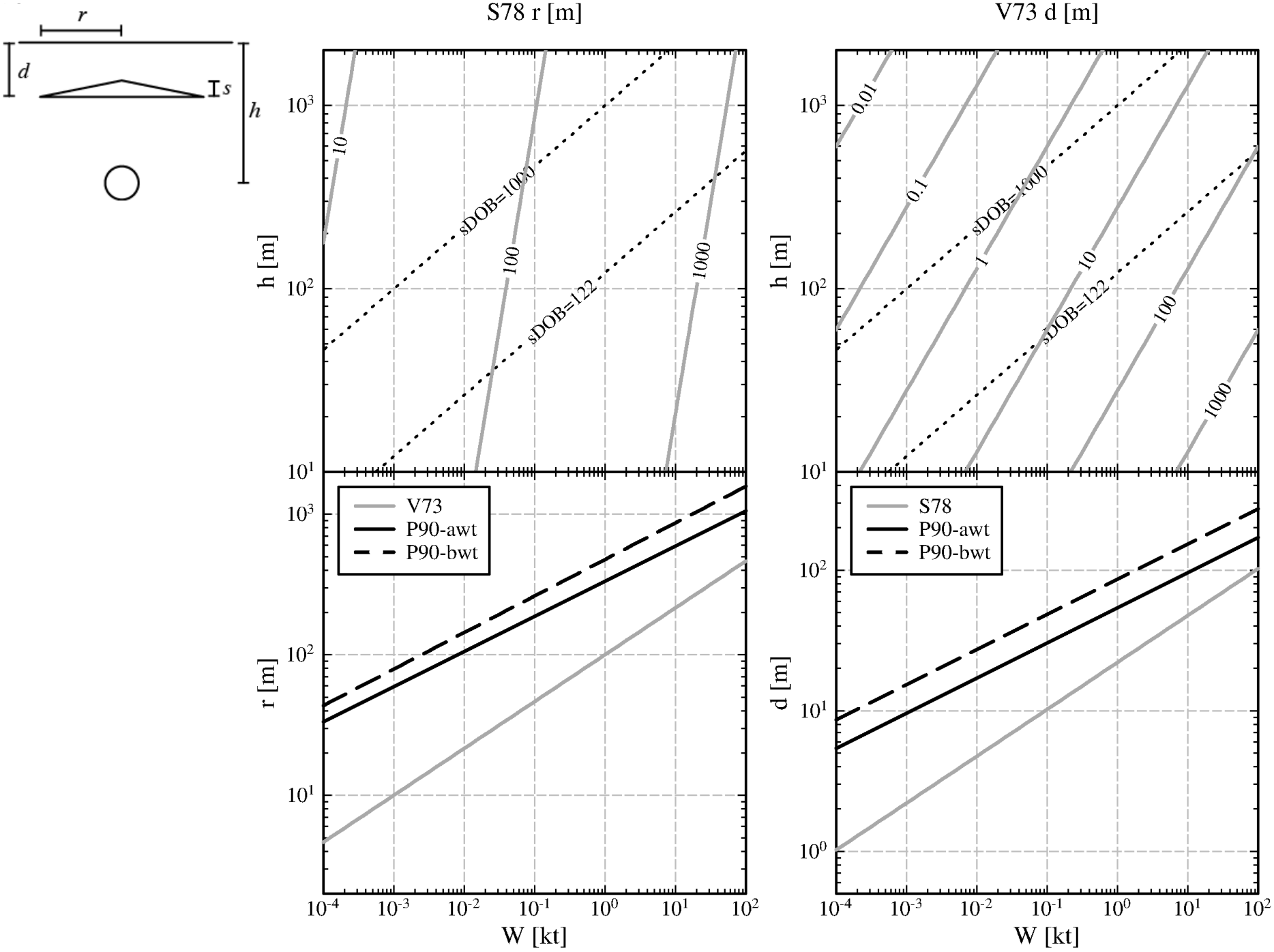
r
d
s
h
S78 r [m]
V73 d [m]
h [m]
10
100
1000
sDOB=1000
sDOB=122
0.01
0.1
1
10
100
1000
sDOB=1000
sDOB=122
V73
P90-awt
P90-bwt
S78
P90-awt
P90-bwt
r [m]
d [m]
W [kt]
W [kt]

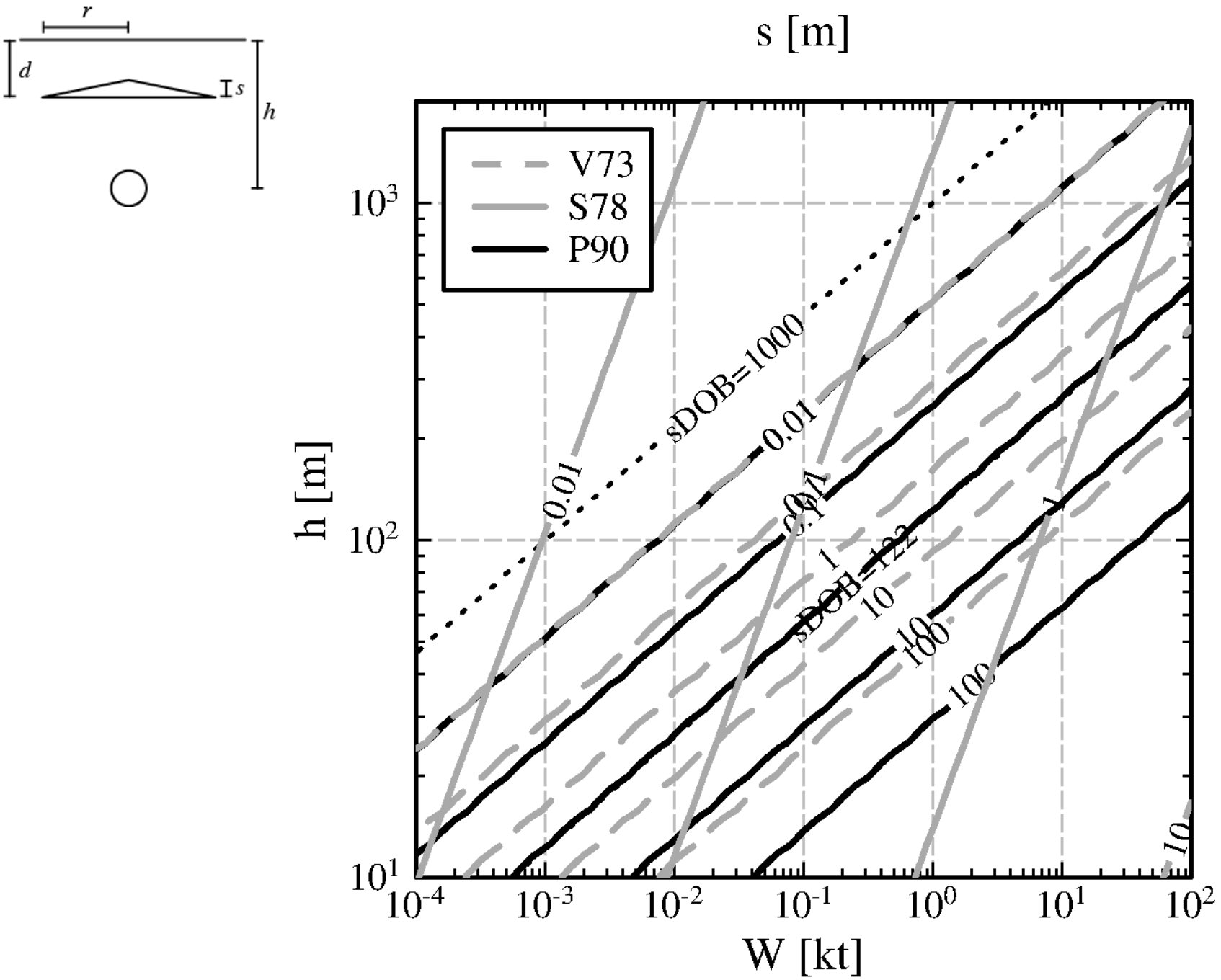
r
d
s
h
s [m]
V73
S78
P90
sDOB=1000
sDOB=122
0.01
0.1
1
10
100
h [m]
W [kt]
10^1
10^2
10^3
10^{-4}
10^{-3}
10^{-2}
10^{-1}
10^0
10^1
10^2

SPE Observations

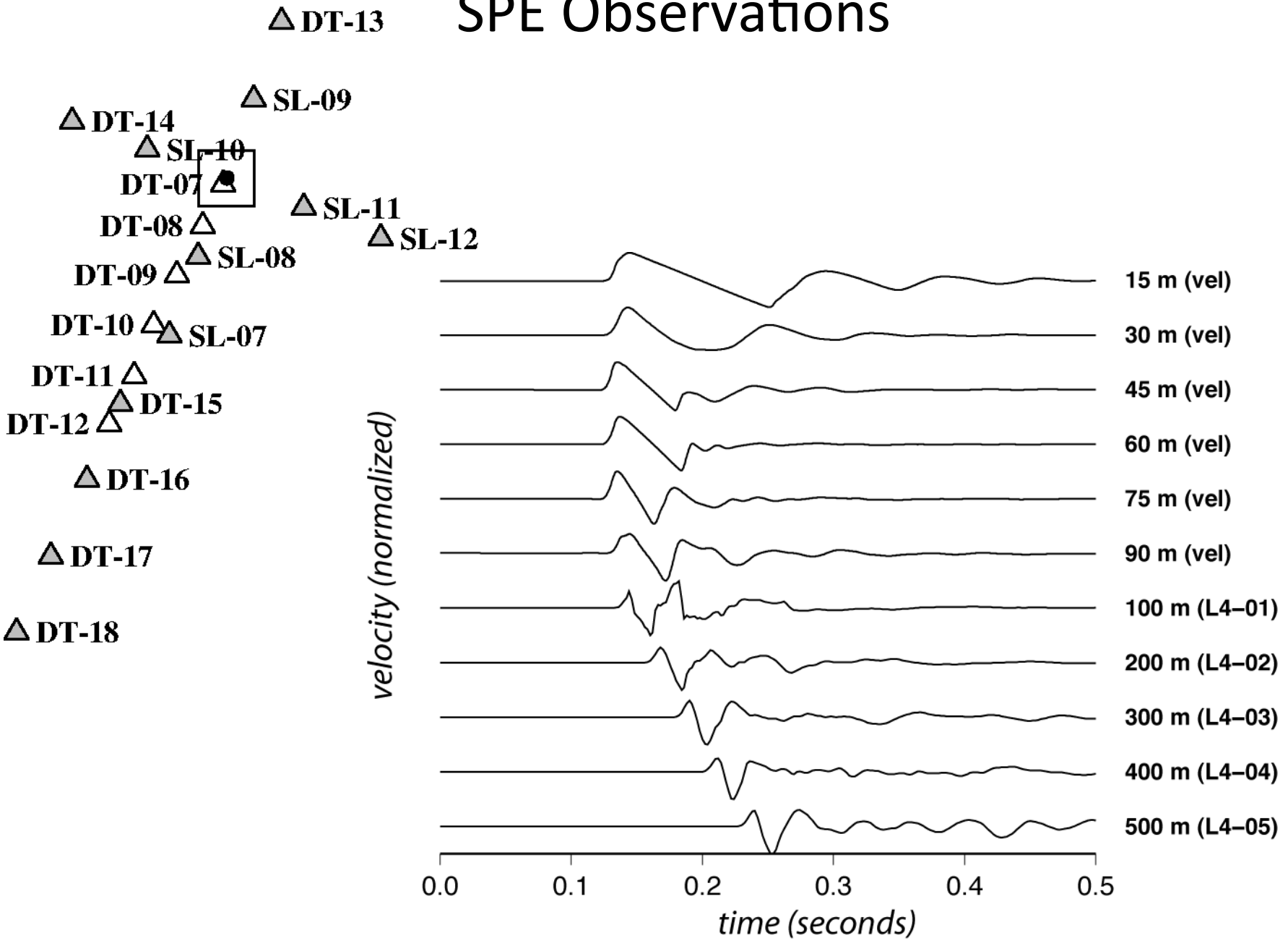

Comparison with PILEDRIVER

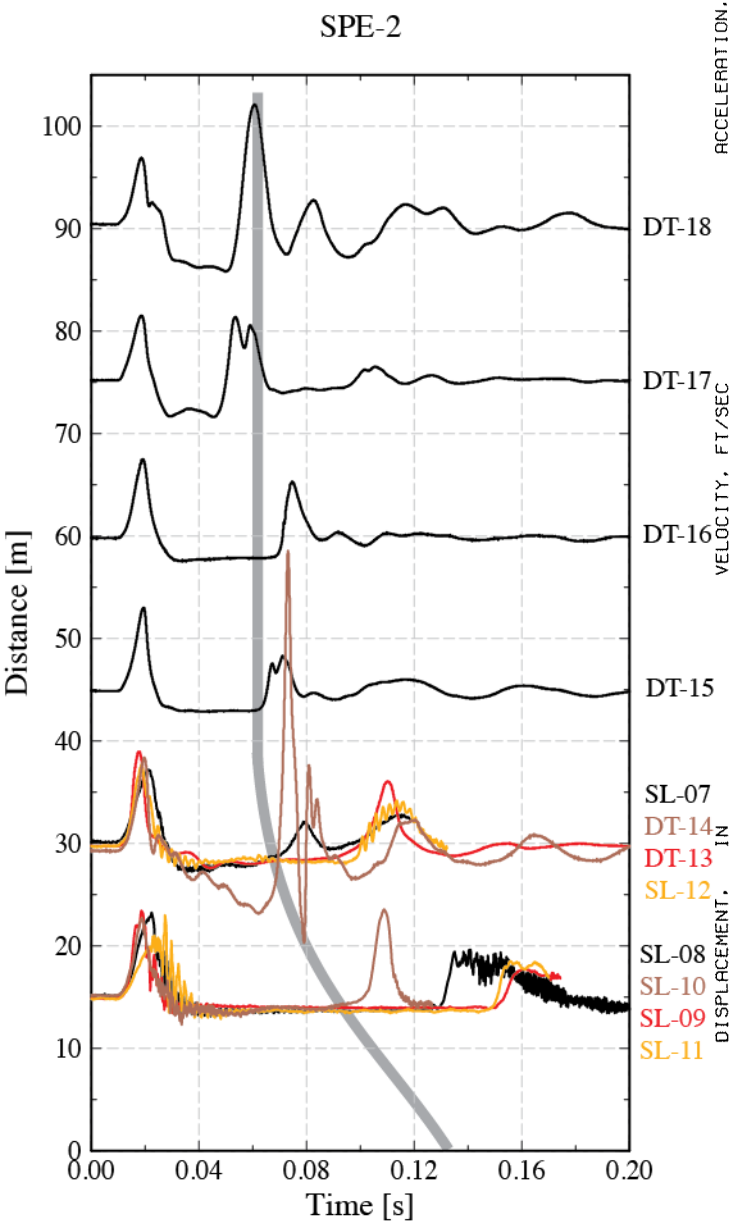

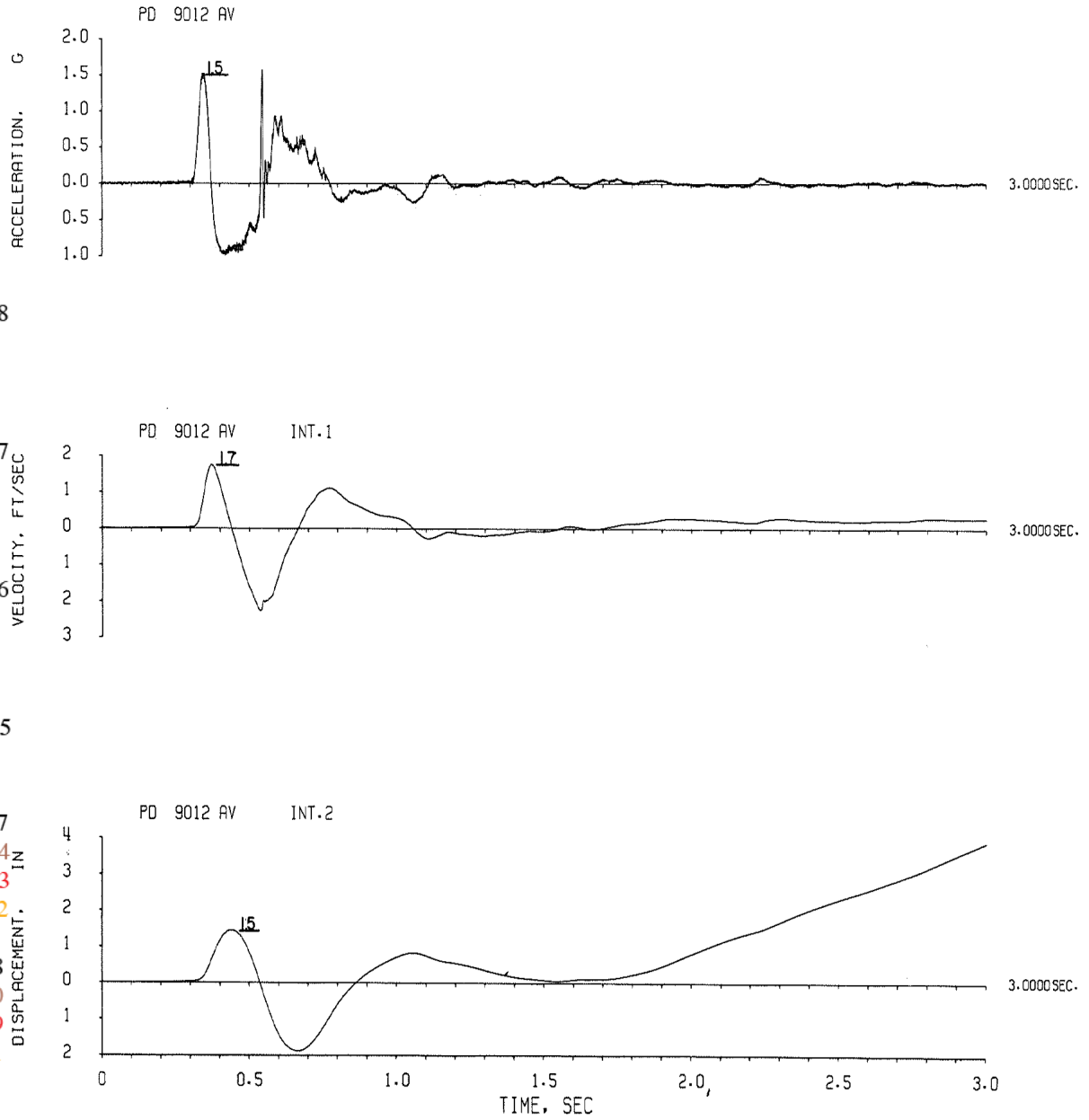

Figure 3.49 Vertical acceleration, velocity, and displacement, 4500 feet horizontal range, 1453 feet above the working point.

Comparison with PILEDRIVER

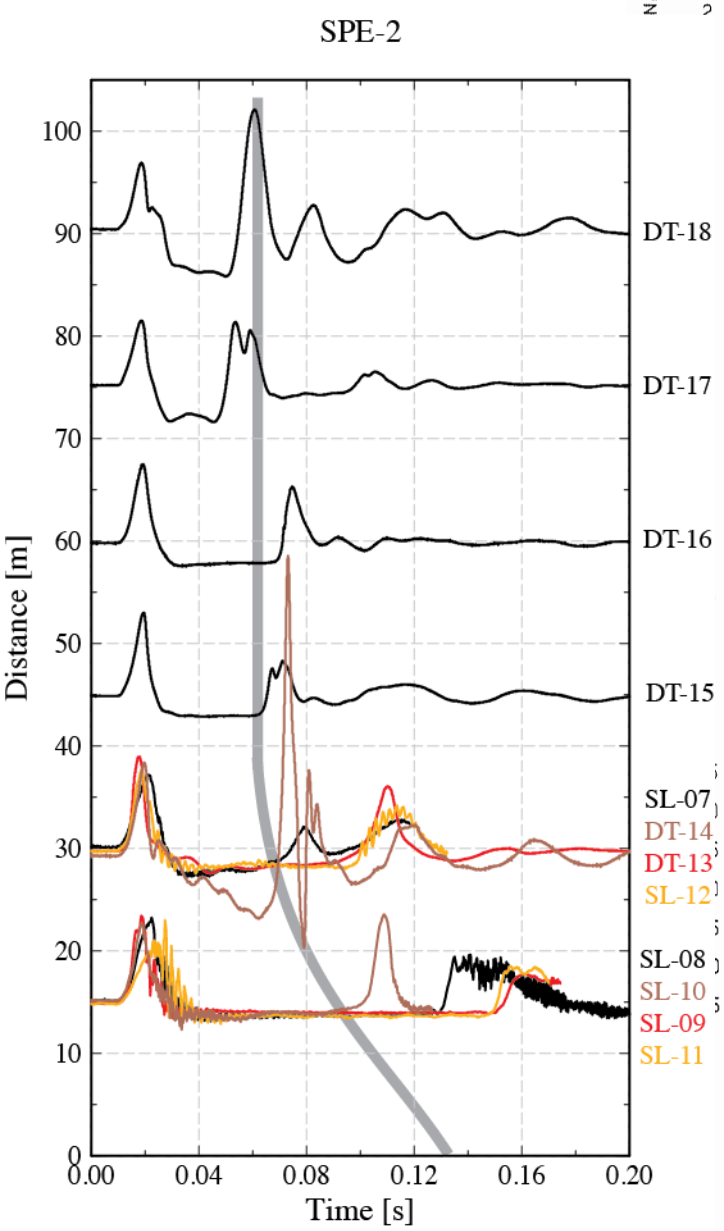

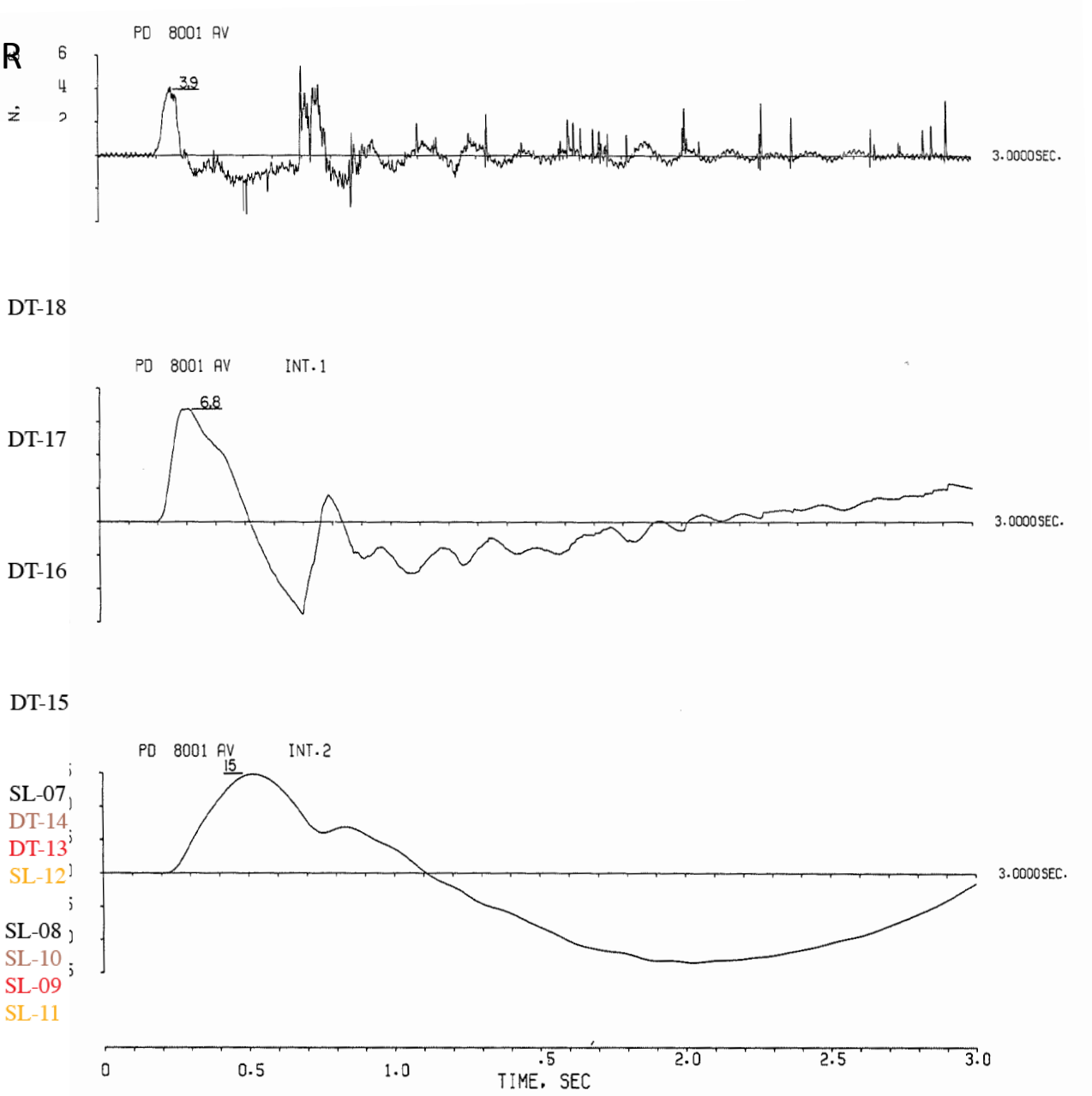

Figure 3.52 Vertical acceleration, velocity, and displacement, C van floor, front.

Comparison with PILEDRIVER

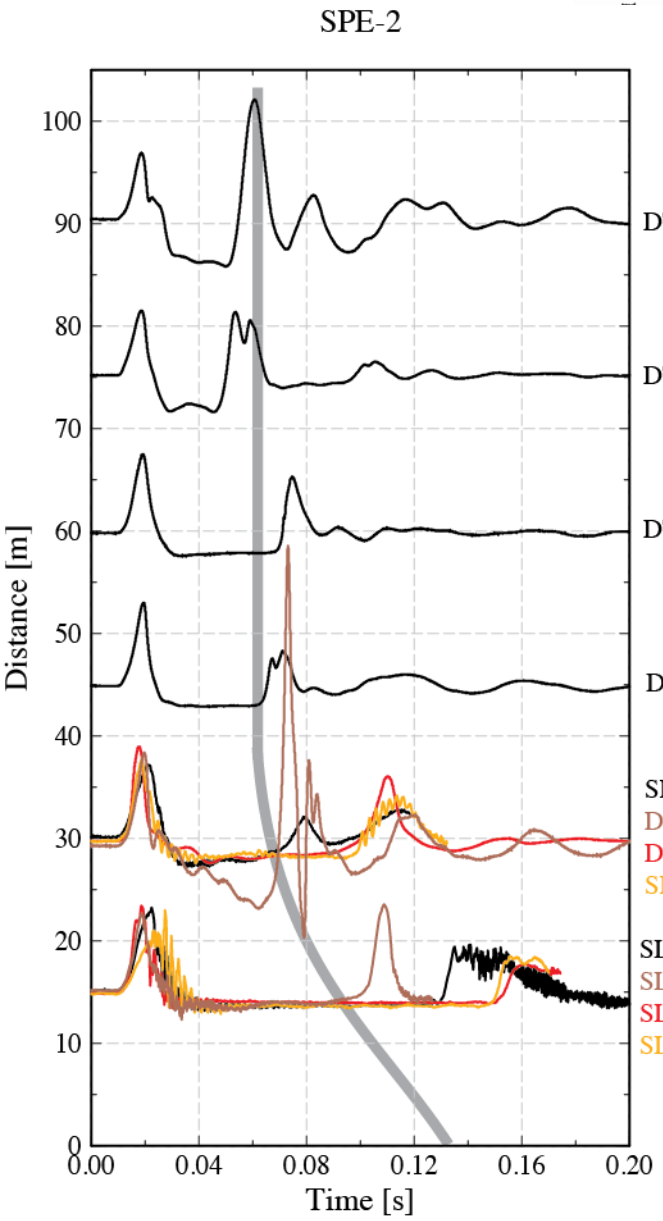

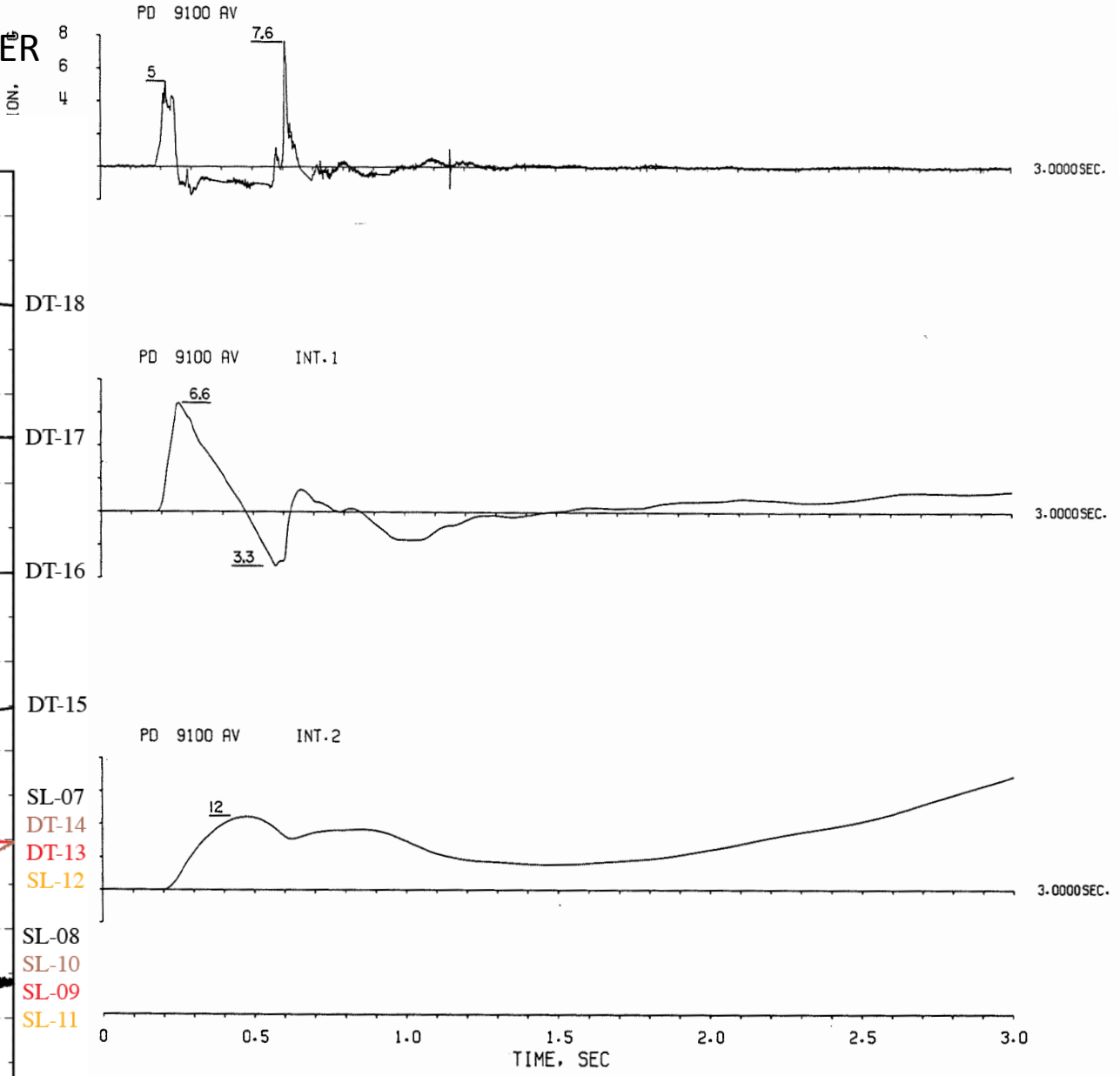

Figure 3.50 Vertical acceleration, velocity, and displacement in trailer park, 1850 feet horizontal range, 1409 feet above the working point.

Comparison with PILEDRIVER

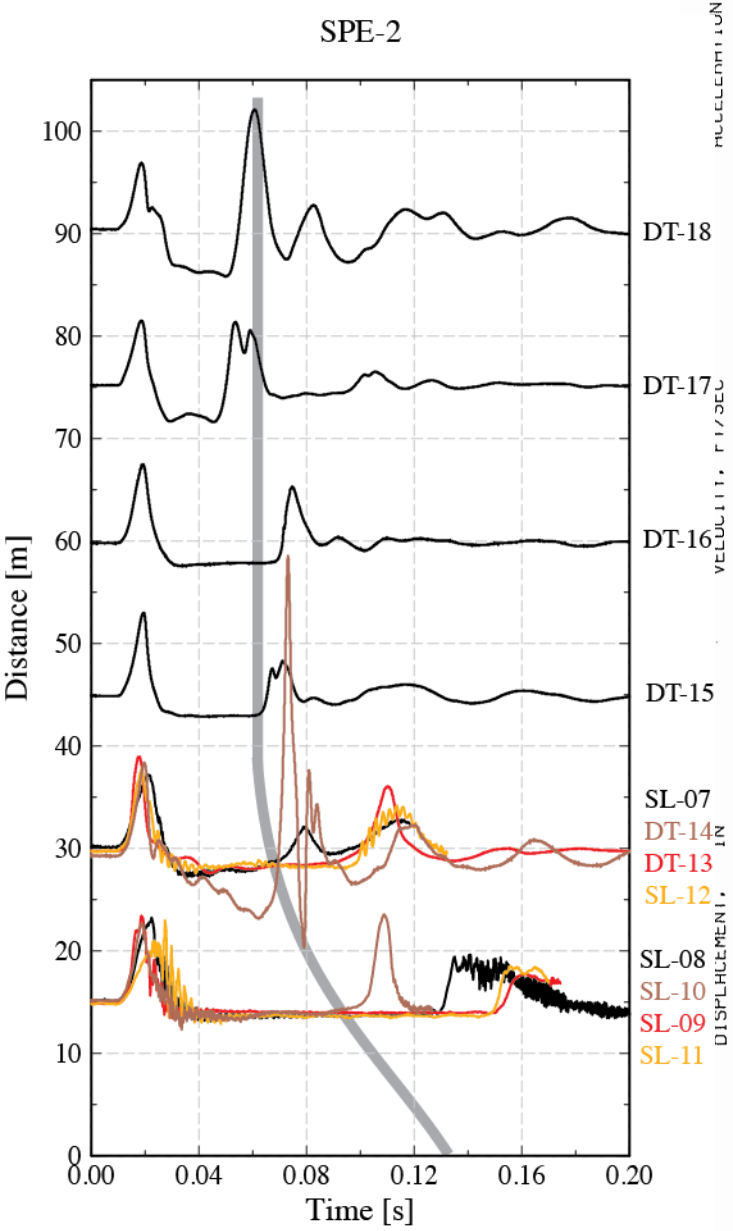

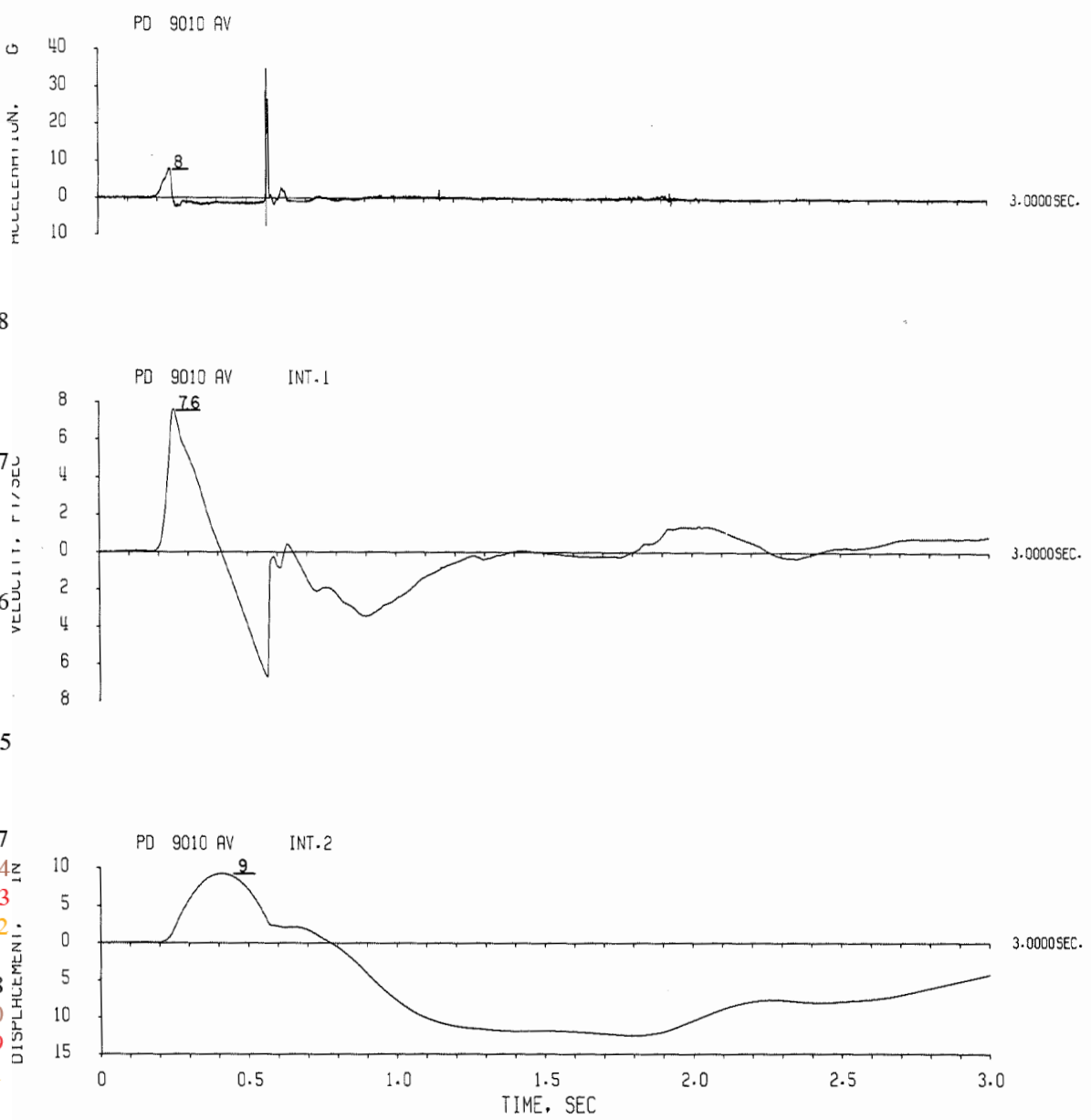

Figure 3.48 Vertical acceleration, velocity, and displacement, 2440 feet horizontal range, 1539 feet above the working point.

Peak GZ velocity

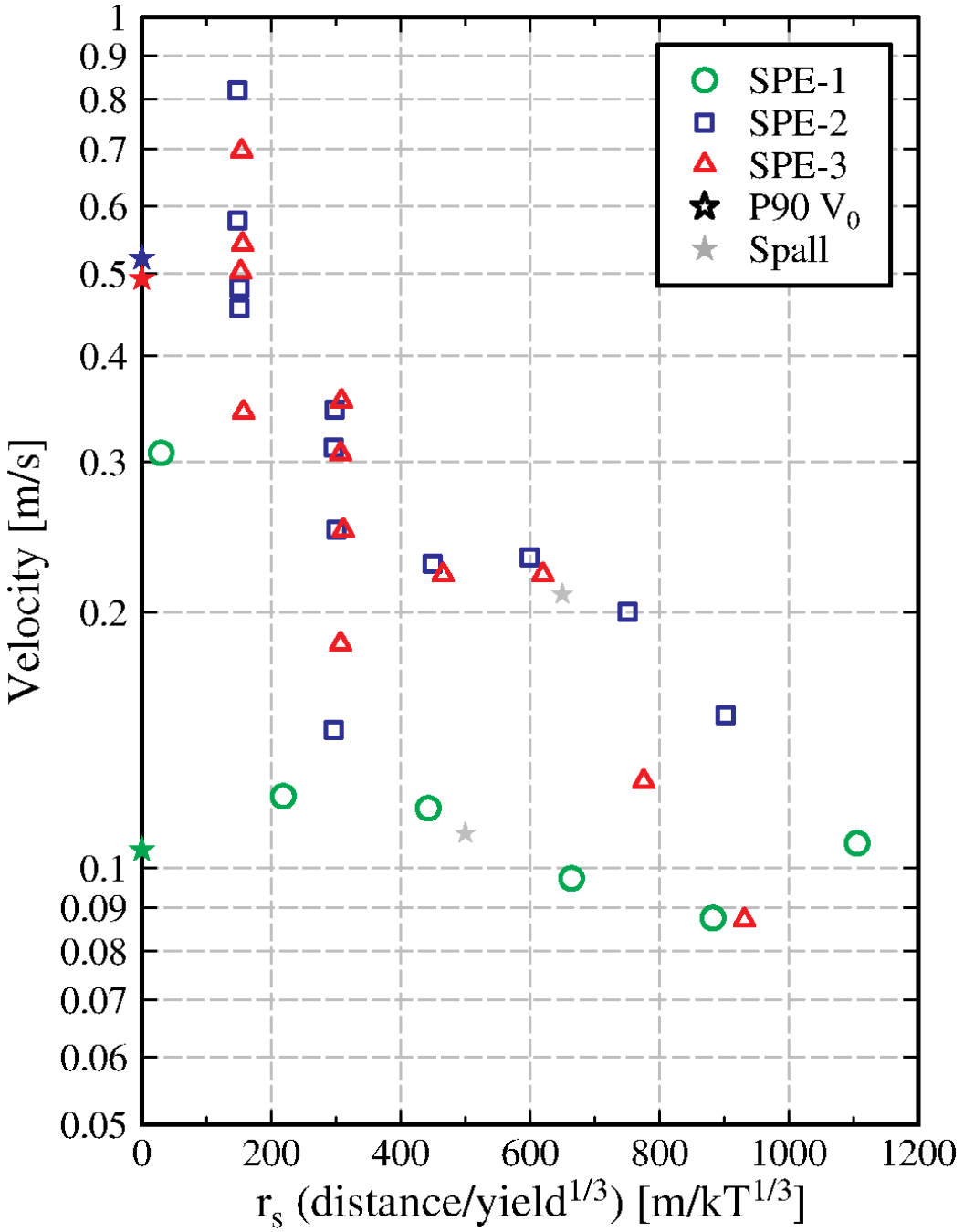

SPE-4 V_0 = 0.05 m/s

Model comparison with SL-10 (15m-NW)

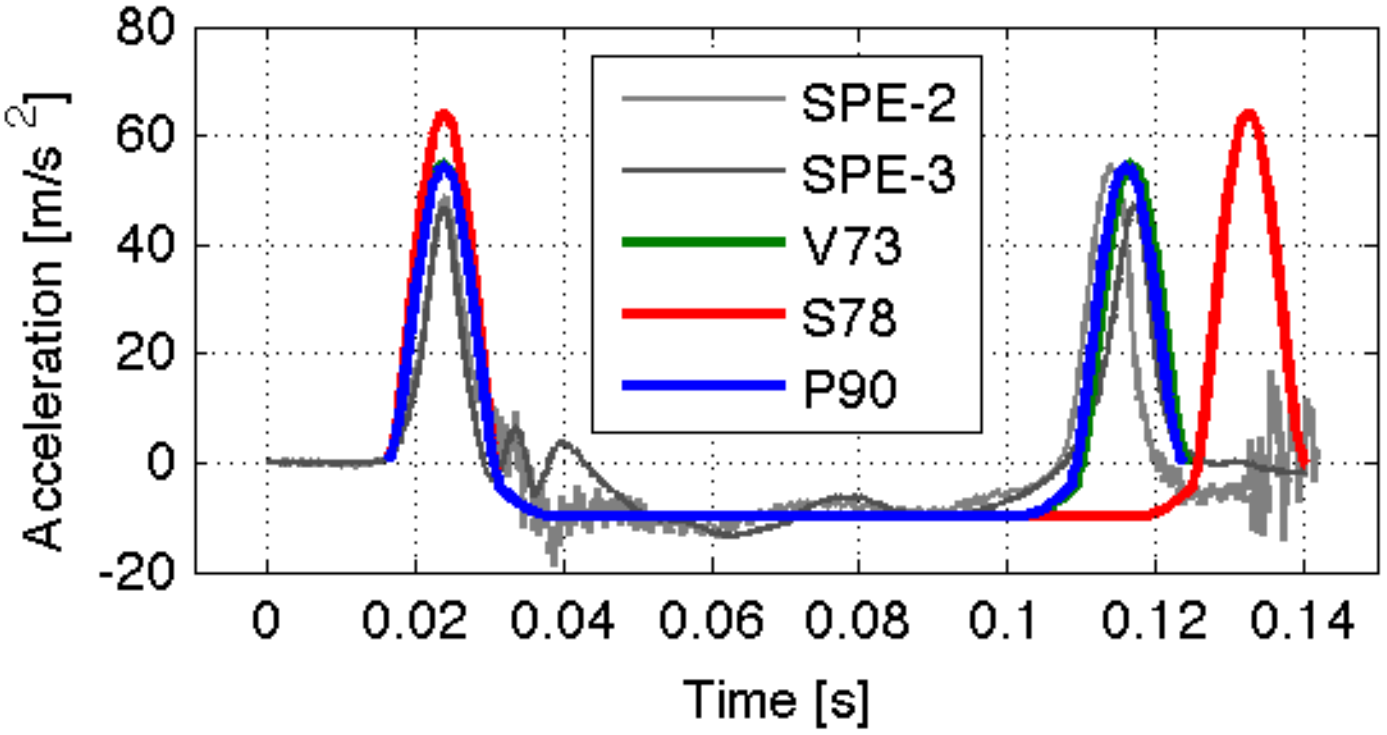

Model	Gap [cm]	Radius [m]	V_0 [cm/s]	Mass [T]	Dwell [ms]	Rise [ms]
V73	1.06	10.00	45.51	2.18	92.9	15.6
S78	1.45	28.72	53.24	24.62	108.7	15.6
P90	1.04	59.39	45.15	75.73	92.2	15.6

Explosion moment and spall force functions

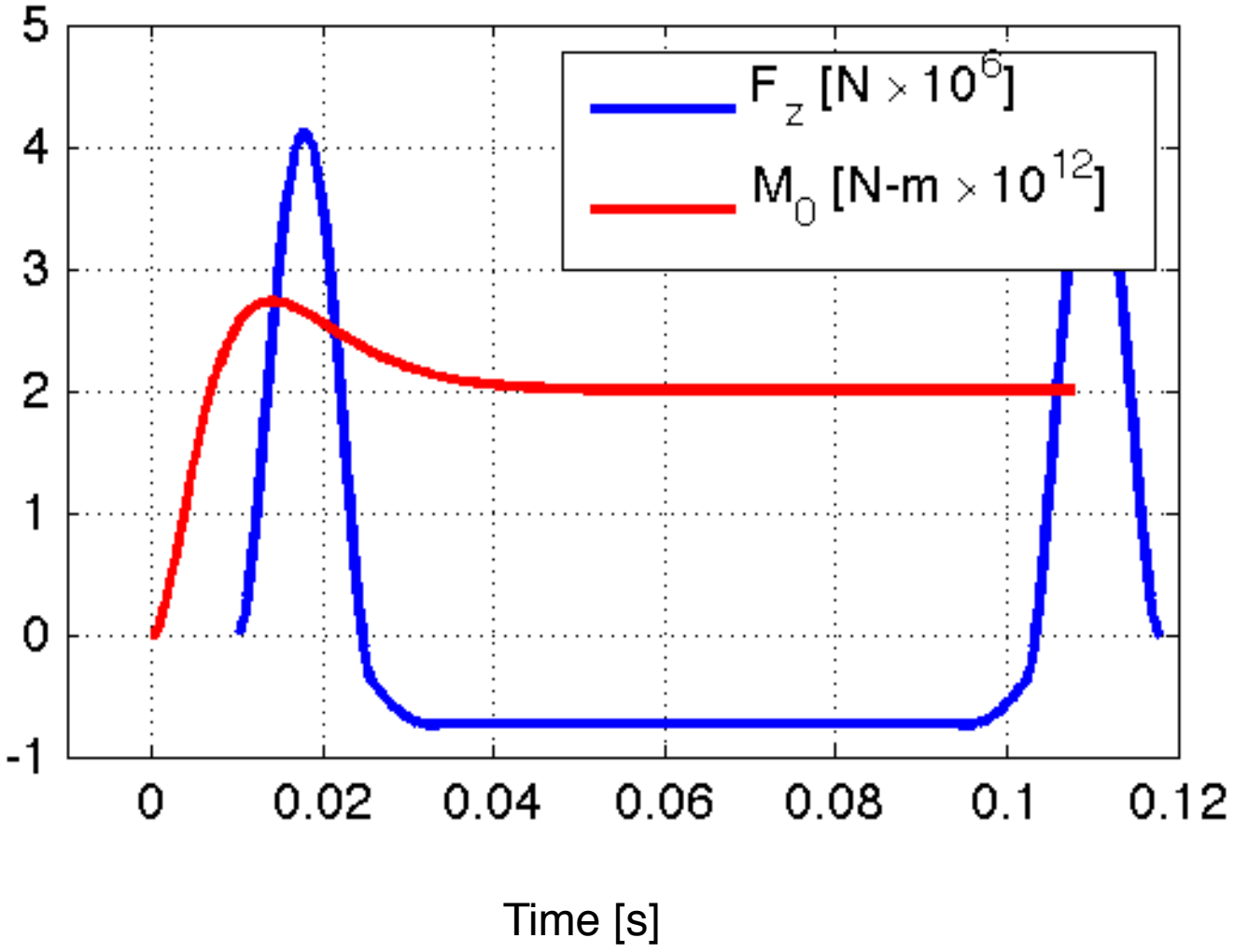

Far-field displacement functions

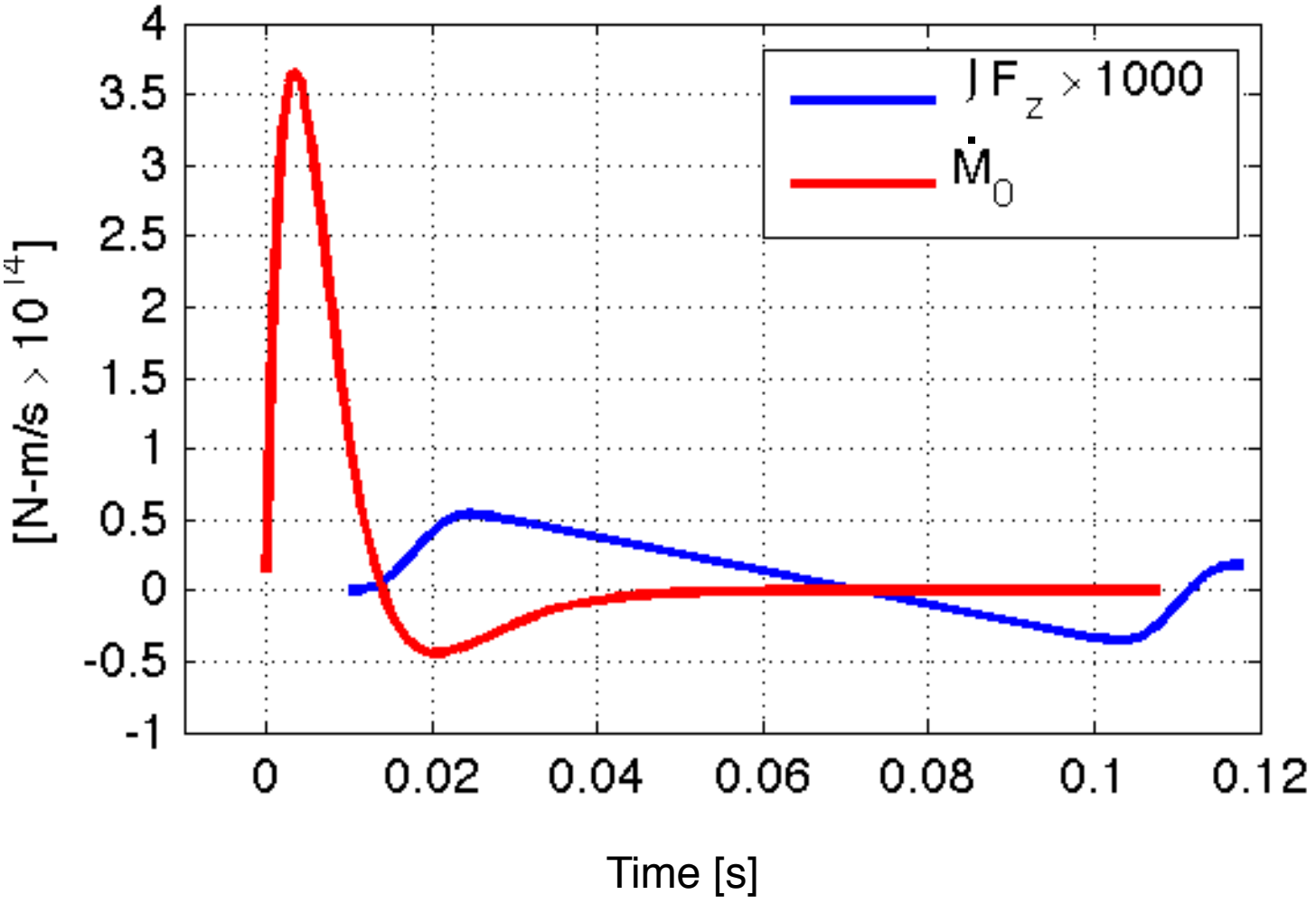

SPE-2/-1 Deconvolution

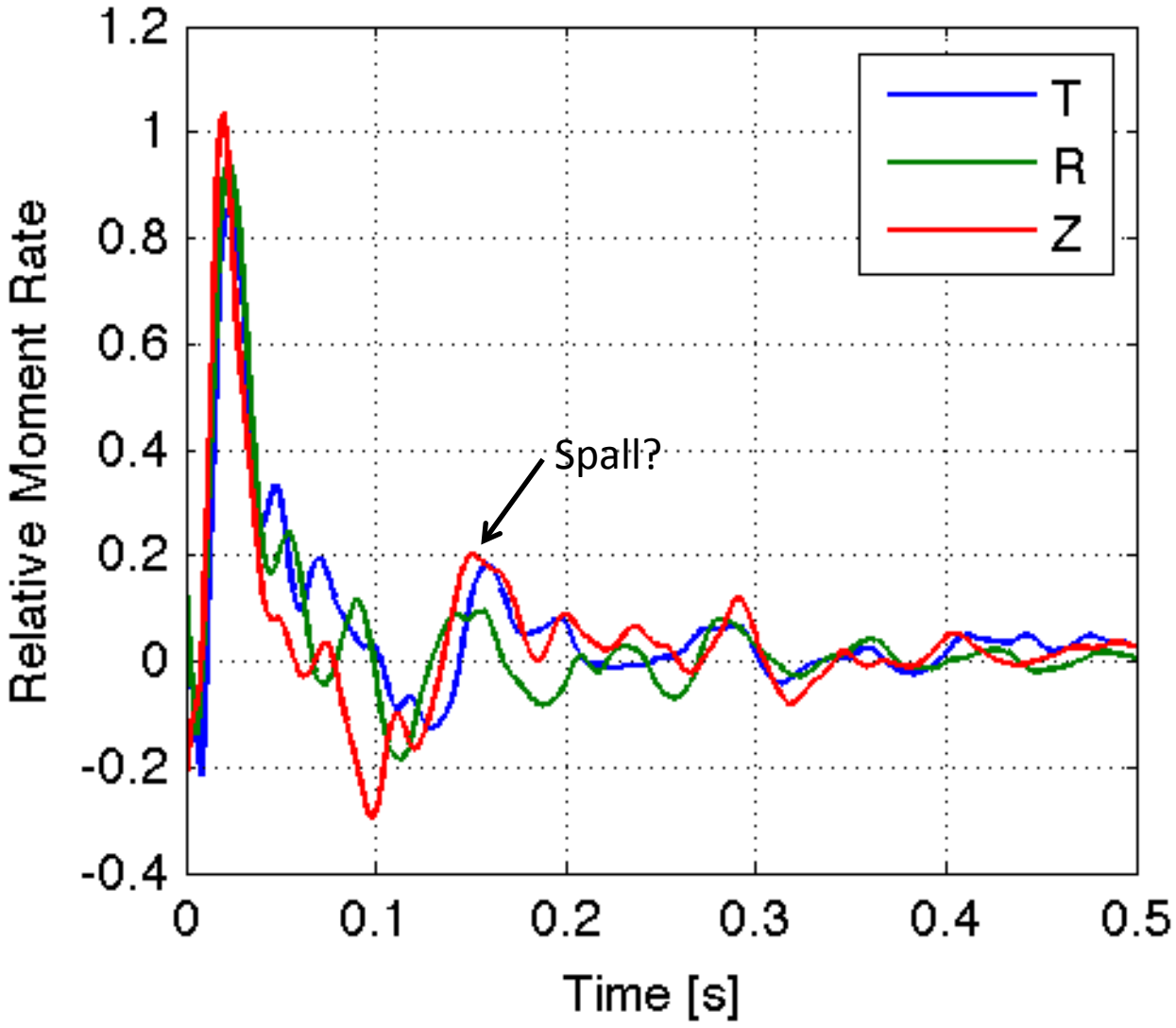

sean@llnl.gov